Supplementary materials

Shared evolutionary trajectories of three independent neo-sex chromosomes in *Drosophila*

Masafumi Nozawa[1,2*], Yohei Minakuchi[3], Kazuhiro Satomura[1,†], Shu Kondo[4,‡], Atsushi Toyoda[3], and Koichiro Tamura[1,2]

[1] Department of Biological Sciences, Tokyo Metropolitan University, Hachioji, Tokyo 192-0397, Japan

[2] Research Center for Genomics and Bioinformatics, Tokyo Metropolitan University, Hachioji, Tokyo 192-0397, Japan

[3] Comparative Genomics Laboratory, Department of Genomics and Evolutionary Biology, National Institute of Genetics, Mishima, Shizuoka 411-8540, Japan

[4] Invertebrate Genetics Laboratory, National Institute of Genetics, Mishima, Shizuoka 411-8540, Japan

[*] Corresponding author: Masafumi Nozawa, manozawa@tmu.ac.jp

[†] Present address: Department of Bio-Science, Nagahama Institute of Bioscience and Technology, Nagahama, Shiga 526-0829 Japan

[‡] Present address: Department of Biological Science and Technology, Faculty of Advanced Engineering, Tokyo University of Science, Katsushika, Tokyo 125-8585, Japan

SUPPLEMENTARY METHODS

Flies

D. americana (strain 15010-0951.03, Millersberg, USA), *D. texana* (strain 15010-1041.00, St. Francisville, USA), and *D. novamexicana* (strain 15010-1031.00, Grand Junction, USA) were obtained from *Drosophila* Species Stock Center (https://www.drosophilaspecies.com/). *D. albomicans* (strain NG-3, Nago, Japan), *D. nasuta* (strain G-86, Curepipe, Mauritius), and *D. kohkoa* (strain X-145, Kuala Lumpur, Malaysia) were originally collected by Osamu Kitagawa and his colleagues from 1977 to 1979 (Kitagawa et al. 1982; Hatsumi et al. 1988) and have been maintained as living stocks at Tokyo Metropolitan University.

DNA extraction, library construction, and sequencing

To remove the effect of bacterial flora in the gut on the *Drosophila* genome sequences as much as possible, we first treated adult flies under a starvation only with water for three days. All survivors were separated into males and females under a stereomicroscope. High molecular weight genomic DNA was extracted from 1-2 g of the males and females separately by using a standard method with proteinase K and phenol (Sambrook and Russell 2001). The DNA was then further purified with Genomic-tip 100/G (QIAGEN, Venlo, Netherlands).

Whole genome shotgun sequencing was performed using the Illumina HiSeq 2500 (Illumina, San Diego) and PacBio RSII/Sequel (Pacific Biosciences, Menlo Park) platforms. For Illumina sequencing, genomic DNA was sheared by a Covaris S2 ultrasonicator (Covaris, Woburn) and then size-selected on an agarose gel using a MinElute Gel Extraction Kit (QIAGEN). A paired-end library with insert size of ~600 bp from each *Drosophila* species (~400 bp for *D. nasuta*) was constructed using a TruSeq DNA PCR-Free LT Sample Prep Kit (Illumina) according to the manufacturer's protocol. Each sequencing

library was run on the Illumina HiSeq 2500 platform with rapid mode. Note that for Illumina sequencing we separately sequenced male and female genomes of *D. albomicans* and *D. americana*, whereas only female genomes were sequenced for *D. nasuta*, *D. kohkoa*, *D. texana*, and *D. novamexicana*. For PacBio sequencing, female genomic DNAs of the six *Drosophila* species were sheared with Covaris G-tubes (Covaris). SMRT bell libraries for *D. albomicans*, *D. nasuta*, and *D. americana* were size-selected using a BluePippin (Sage Science, Beverly) with 15-17 kb cut-off. Sequencing run was performed on the PacBio RSII system using P6/C4 chemistry for 6 hours. A 20-kb library for *D. texana* and two 30-kb libraries for *D. kohkoa* and *D. novamexicana* were run on the PacBio Sequel system using Binding Kit1.0/Sequencing Kit1.2.1 for 6 hours and Binding Kit2.0/Sequencing Kit2.0 for 10 hours, respectively. See Table S1 for data summary.

Genome assembly

For *D. albomicans*, *D. nasuta*, and *D. americana*, PacBio long reads were assembled *de novo* using the Hierarchical Genome Assembly Process (HGAP) 3 (Chin et al. 2013) in the SMRT Portal (Pacific Biosciences). For *D. kohkoa*, *D. texana*, and *D. novamexicana*, the HGAP4 in SMRT Link (Pacific Biosciences) was used. Illumina sequence reads were then mapped onto the assembled genomes using BWA mem (v0.7.7) with default settings (Li and Durbin 2009). Mismatches and indels between the PacBio assembly and Illumina reads were detected by samtools (0.1.19) and replaced if they were supported by ≥80% of the reads, ≥10 reads, and reads from both directions. All contigs were then screened by the Public database to detect contaminants and mitochondrial sequences. More specifically, using the contigs as queries, we conducted a homology search (BLASTN ver. 2.2.9) against (a) genome sequences of bacteria, archaea, and fungi in the RefSeq database, (b) the mitochondrial genome of the target *Drosophila species*, and (c) the genome sequence of *D. melanogaster* with cut-off a e-value of 10^{-10}.

The contigs that met the following two criteria were removed as contaminants. (1) Equal to or more than 1% of a contig in length is hit to either (a) or (b). (2) Equal to or more than 1% of a contig in length is not hit to (c). Assembly statistics is given in Table S2.

For each of the genome assemblies of the six species as well as the assembly of *D. obscura* (Nozawa et al. 2016), we next assigned each contig to a chromosome (a Muller element) as follows. (1) By using all amino-acid sequences (dmel-all-translation-r6.27.fasta from FlyBase) in *D. melanogaster* as queries, TBLASTN ver. 2.9.0+ (Altschul et al. 1997) was conducted against all contigs in a genome assembly as a database. (2) For each contig region, a best-hit query gene with the lowest e-value was determined. (3) The chromosome number (and the Muller element) on which the gene is located was extracted. 4) If a contig contains 10 or more genes homologous to *D. melanogaster* and more than two-thirds of the genes are located on a same Muller element in *D. melanogaster*, we regarded that the contig is a part of the chromosome (Muller element). All other contigs were classified as unassigned (NA).

For *D. miranda*, we mapped the Illumina sequence reads from the strain 14011-0101.17 (Nozawa et al. 2016) onto the reference genome assembly (D.miranda_PacBio2.0 retrieved from NCBI) by using BWA mem (ver. 0.7.17) (Li and Durbin 2009). Using GATK (ver. 3.7.0) (DePristo et al. 2011), we then detected all variants if the site is homozygous for alternative allele with a minimum coverage of 5× and genotype quality of 20. For autosomes and X, both female and male reads were used to detect variants. For neo-X and neo-Y, only female and male reads were used, respectively. Replacing the nucleotides in the reference genome with the variants detected, we obtained a "pseudo-reference" genome sequence of the strain 14011-0101.17 of *D. miranda*. For *D. pseudoobscura*, we used the available genome assembly (dpse-all-chromosome-r3.1.fasta) on FlyBase (https://flybase.org/).

To obtain the neo-Y assemblies of *D. americana* and *D. albomicans*, we first filtered out adapter sequences and low quality nucleotides from all reads from Illumina sequencing by using Cutadapt 2.8

(Martin 2011) and SolexaQA++ v3.1.7.1 (Cox et al. 2010), respectively, and selected read pairs with quality value ≥25 and ≥50-nucleotide long. Those selected read pairs from female and male DNAs were then separately mapped onto the genome assembly obtained above by using BWA mem (ver. 0.7.17) (Li and Durbin 2009). After calling variants by GATK (ver. 3.7.0) (DePristo et al. 2011), if the allele at a nucleotide position on neo-X is heterozygous in males but homozygous for the reference allele in females, the allele that is not detected in females was regarded as the neo-Y allele. When the allele at a position is heterozygous in males but none of them were shared with the allele in females, the allele with the highest frequency was used as the plausible nucleotide on the neo-Y (only 55 and 26 such sites in *D. albomicans* and *D. americana*, respectively). Finally, using an in-house perl script (see *SUPPLEMENTARY CODE*), neo-Y sequences were obtained by replacing neo-X sequences with those male-specific variants of read depth ≥5 and genotype quality ≥20. See Table S2 for the stats of the genome assemblies in this study.

The genome assemblies of the nine species used in this study were evaluated by BUSCO (benchmarking universal single-copy orthologs) ver. 4.0.2 software (Simao et al. 2015) with the "diptera_odb10" dataset containing 3,285 BUSCOs (Table S3).

RNA extraction, library construction, and sequencing

Third instar larvae (before wandering), pupae (48-60 hours after pupation), adults (72-96 hours after eclosion), ovaries (10-14 days old after eclosion), and testes (10-14 days old after eclosion) of *D. albomicans*, *D. nasuta*, *D. kohkoa*, *D. americana*, *D. texana*, and *D. novamexicana* were used for RNA extraction. Total RNA from each tissue (5 individuals, but ~20 individuals for ovaries and testes) was extracted using PureLink RNA Mini Kit (Thermo Fisher Scientific, Waltham) for males and females separately. mRNA was further purified from the total RNA using the NEBNext Poly(A) mRNA Magnetic Isolation Module (NEB, Ipswich). cDNA libraries were then constructed from mRNA using the NEBNext

Ultra Directional RNA Library Prep Kit for Illumina or NEBNext Ultra II Directional RNA Library Prep Kit for Illumina (NEB). Paired-end sequencing of 101 or 151 bp was performed by Macrogen (Seoul, South Korea) with HiSeq 4000 or HiSeq X, respectively. To take fluctuation among samples into account, two independent experiments were conducted for each condition (i.e., two biological replicates were made for each condition). For *D. miranda*, *D. pseudoobscura*, and *D. obscura*, we used the data from Nozawa et al. (2016). See Table S4 for data summary.

Transcriptome assembly

To assemble the transcriptome sequence for the nine species, we used female and male RNA-seq data from 3rd instar larvae, pupae, and adults. First, all reads were processed with Cutadapt and SolexaQA++ as mentioned above to remove adapter and low quality sequences. All qualified read pairs from each sample were then mapped onto the genome assembly obtained by using HISAT2-2.1.0 (Kim et al. 2019) and processed with StringTie 1.3.6 (Pertea et al. 2015) to predict the transcriptome for each species.

Gene annotation

For expressed genes (i.e., the predicted transcripts), we used TransDecoder-5.5.0 (Haas et al. 2013) to predict coding sequences within each transcript with all amino-acid sequences in *D. melanogaster* (dmel-all-translation-r6.27.fasta retrieved from FlyBase) as guide sequences. We also predicted genes in each genome *ab initio* by using Augustus-3.3.2 (Stanke and Waack 2003) with the option of --species=fly. See Table S5 for the summary of annotated genes. For *D. albomicans* and *D. americana*, if (1) the coding sequences of a homolog on neo-X and neo-Y are completely identical and (2) the male to female coverage ratio of Illumina short reads on the corresponding neo-X positions is within

the bottom 2.5 percentile (i.e., 0.52 for *D. albomicans* and 0.77 for *D. americana*) in the ratio of all nucleotides on autosomes, we regarded that the neo-Y region corresponding to the neo-X homolog is too diverged for neo-Y-derived reads to be mapped, which may have resulted in the identical sequences of neo-X and neo-Y and low male to female coverage ratio. Therefore, we remove these homologs from all analyses.

Estimation of gene expression level

All qualified read pairs were mapped onto the genome assembly for each species using STAR 2.7 (Dobin et al. 2013) with the gtf file of the transcriptome sequence obtained above. The mapped data were further processed with RSEM v1.3.1 (Li and Dewey 2011) to obtain FPKM (fragments per kilobase of exon per million mapped reads, Mortazavi et al. 2008) and TPM (transcripts per kilobase million mapped reads, Wagner et al. 2012) for each gene. When we compared the gene expression level among samples from different species, we normalized the FPKM value for each gene by dividing by the median of the FPKM values of a sample (corrected FPKM or cFPKM, Lin et al. 2012) to remove statistical biases as much as possible. When the gene expression level was compared among samples from different species, we also normalized the TPM by dividing by the median of the TPM values (corrected TPM or cTPM). For within-species comparisons, we used TPM as it is. The mapping rate for each sample is shown in Table S21.

Identification of orthologs and paralogs

To identify orthologs in the three closely related species (i.e., *D. miranda-D. pseudoobscura-D. obscura*, *D. albomicans-D. nasuta-D. kohkoa*, or *D. americana-D. texana-D. novamexicana*), we conducted homology search using BLASTP ver. 2.9.0+ (Altschul et al. 1997). If a gene from each species

was a reciprocal best-hit in all combinations of the species, the genes were regarded as an ortholog. It should be mentioned that when a gene was missing in one species, the remaining genes were still regarded as an ortholog if they were reciprocal best-hits each other.

To identify inparalogs that emerged by gene duplication after splitting from closely related species, we conducted a homology search (BLASTP ver. 2.9.0+) by using all genes in one species (species 1, e.g., *D. miranda*) as queries, against the database in which all genes in the species (species 1) and its closely related species (species 2, e.g., *D. pseudoobscura*) were included. For each query, we regarded all species 1 genes that showed lower e-values than the e-value for the species 2 gene (i.e., the ortholog) as inparalogs. Note that for the query genes located on neo-X and neo-Y, we excluded the genes on neo-Y and neo-X, respectively, from the database, because they are not derived from gene duplication but diverged through sex chromosome differentiation. In this way, all genes were classified into 1:1:1 orthologs without paralogs (sometimes missing in one species), other orthologs containing inparalogs, and species-specific genes.

Gene classification

To check the integrity of the coding sequence for each gene, we conducted a following procedure. (1) If either initiation or stop codon was missing in a gene due to the presence of at least one ambiguous site (i.e., N) in the flanking 100 nucleotides or the location of the gene at the end of contigs/scaffolds of the assembly, the gene was regarded to be 'unclassified'. (2) If either initiation or stop codon was missing in spite of no ambiguous site in the flanking 100 nucleotides nor the location at the end of contigs/scaffolds, the gene was regarded to be 'disrupted'. For remaining genes in which both initiation and stop codons are present: (3) If a gene had a homolog in *D. melanogaster* with a cut-off e-value of 10^{-20} by BLASTP search, the nucleotide sequence of the gene was aligned with that of the *D. melanogaster*

homolog by using MACSE v2.03 (Ranwez et al. 2018) that accounts for frameshifts and internal stop codons. If either frameshifts or internal stop codons were detected in the nucleotide sequence of the gene, the gene was regarded as being 'disrupted'. However, if frameshifts or internal stop codons were detected in the sequence of the *D. melanogaster* gene, the gene in the target species was regarded as being 'unclassified'. (4) If a gene did not have a homolog in *D. melanogaster* but a homolog is present in the closely related species (e.g., *D. pseudoobscura* or *D. obscura* for *D. miranda*), we aligned these sequences by MACSE as mentioned above with some manual adjustment. If either frameshifts or internal stop codons were detected in the nucleotide sequence of the gene, the gene was regarded as being 'disrupted'. (5) If a gene did not have any homolog in closely related species, the coding sequence of the gene was translated into amino-acid sequence. If an internal stop codon was detected, the gene was regarded as being 'disrupted'. (6) All remaining genes were regarded as being 'intact'.

To check the expression potential for each gene, we used the following criteria. (7) If a gene (or a transcript of a gene, strictly speaking) was identified by the HISAT-StringTie pipeline, the gene was regarded as being 'expressed'. (8) For the genes that were not detected by the HISAT-StringTie pipeline but predicted by Augustus, if the gene showed the FPKM value of ≥ 1 in at least one tissue examined, the gene was regarded to be 'expressed'. (9) All other genes were regarded as being 'non-expressed'.

Finally, if a gene is 'intact' and 'expressed', the gene was regarded as 'functional'. If a gene is 'disrupted' and 'expressed', the gene was regarded to be 'disrupted'. If a gene is 'intact' and 'non-expressed', the gene was regarded as being 'silenced'. If a gene is 'disrupted' and 'non-expressed', the gene was regarded to be 'silenced and disrupted'. All remaining genes were regarded as 'unclassified'.

Estimation of the extent of dosage compensation

For this analysis, we used only the orthologs that have no inparalogs in any of each trio (i.e., *D. miranda-D. pseudoobscura-D. obscura*, *D. albomicans-D. nasuta-D. kohkoa*, or *D. americana-D. texana-D. novamexicana*) and are located on the same Muller elements in all three species from each trio. In addition, for autosomal and X-linked genes we only used the orthologs that are functional in the three species. For the Muller element that became neo-sex chromosomes, we also analyzed the orthologs that were pseudogenized or deleted on neo-Y.

To examine the level of DC for each gene, we used R_{Lin} (Lin et al. 2012). The equation of R_{Lin} can be written as

$$R_{\mathrm{Lin}} = \frac{\mathrm{cFPKM}_{\mathrm{neo-X,tar}} / \mathrm{cFPKM}_{\mathrm{proto-X,com}}}{\mathrm{median\_cFPKM}_{\mathrm{A/X,tar}} / \mathrm{median\_cFPKM}_{\mathrm{A/X,com}}},$$

where cFPKM is the corrected number of fragments per kilobase of exon per million mapped fragments, which linearly adjusted an individual FPKM to make the median expression identical to 1. Subscripts tar, com, neo-X, proto-A, and A/X denote target species (e.g., *D. miranda*), comparing (or different) species (e.g., *D. pseudoobscura*), the neo-X Chromosome, an autosome orthologous to the neo-X in comparing species (e.g., the Chromosome 3 in *D. pseudoobscura*), and autosomes/canonical X, respectively. The essence of this equation is to detect changes in male expression between species due to the emergence of sex chromosomes using expression change of autosomal and X-linked genes as a control. If there is no DC, the R_{Lin} value will be 0.5 because males of target species have only one copy of the neo-X whereas males in comparing species carry two copies. In contrast, the value is expected to be 1 if DC is perfect. We used the cFPKM and the cTPM values as indices of gene expression and check the consistency between the indices.

Note that in the original R_{Lin}, the ratio of expression of a target gene on neo-X in a species (e.g., neo-X in *D. miranda*) to its ortholog on the orthologous autosome in its close relative (e.g., Chromosome

3 in *D. pseudoobscura*) is normalized by the median ratio of expression of all genes on autosomes (see Nozawa et al. 2018 for an equation). However, we used not only autosomal genes but also X-linked genes in both species for normalization, because genes that are located on autosomes or X in both species should theoretically show the same expression level. It should be mentioned that in this study, we used the cFPKM value as an index of gene expression following the original method (Lin et al. 2012) to consider the statistical bias of using the FPKM as much as possible (Wagner et al. 2012). We also used cTPM to check the consistency of our results.

Neo-X-linked and neo-Y-linked genes were classified into four categories depending on the functionality. If a neo-X-linked and a neo-Y-linked homolog are both functional, the homolog was classified into a X_F-Y_F gene (i.e., a subscript F indicates functional genes). If a neo-X-linked gene is functional but its neo-Y-linked homolog is a pseudogene, the homolog was grouped into a X_F-Y_P gene (i.e., a subscript P indicates pseudogenes). Similarly, homologs can be classified into X_P-Y_F and X_P-Y_P genes. To test gene-by-gene DC, the R_{Lin} values for X_F-Y_P and X_F-Y_F genes were statistically compared by Mann-Whitney *U* test with the correction of multiple testing by the Benjamini and Hochberg method (Benjamini and Hochberg 1995).

Estimation of pseudogenization events

We estimated the number of pseudogenization events on each lineage based on the parsimony principle using the gene classification (functional, silenced, disrupted, silenced and disrupted, and unclassified) as mentioned above. For this analysis, we used only the orthologs that are located on the same Muller elements during the evolution of the three species considered, do not have any inparalogs, and functional in the outgroup species (e.g., *D. obscura*, *D. kohkoa*, and *D. novamexicana* for *D. miranda*, *D. albomicans*, and *D. americana*, respectively). For example, if a gene is functional, silenced, disrupted,

and functional on the *D. miranda* neo-X, the *D. miranda* neo-Y, the *D. pseudoobscura* Chromosome 3, and the *D. obscura* Muller element C, respectively, a pseudogenization event for the ortholog is inferred both on the neo-Y and the *D. pseudoobscura* lineages.

The pseudogenization rates between lineages were compared by χ^2 test. The expected numbers of pseudogenization events on the two lineages were computed by multiplying the total number of pseudogenization events on the two lineages by the ratio of the evolutionary time of one lineage to the sum of the evolutionary times of the two lineages. For example, the number of pseudogenization events on the ancestral lineage of the neo-sex chromosomes in *D. miranda* is 31, whereas that on the neo-X lineage is 123. Since the evolutionary time for each lineage is 0.9 and 1.1 Myrs, respectively, the expected number of pseudogenization events on the former and the latter lineages under the equal rate of pseudogenization are $(123+31) \times 0.9/2.0 = 69.3$ and $(123+31) \times 1.1/2.0 = 84.7$, respectively.

Estimation of evolutionary distance on each branch

To clarify the functional constraints on neo-X, neo-Y, and its ancestral lineages, we computed the nonsynonymous and synonymous nucleotide divergence per site for each branch of the tree from the three species considered. For this analysis, we used only the orthologs that are located on the same Muller elements during the evolution of the three species considered, do not have any inparalogs, and functional in the outgroup species as mentioned above. Coding sequences for each ortholog were translated into amino-acid sequences and aligned by Muscle v3.8.31 (Edgar 2004). The aligned amino-acid sequences were reversed to nucleotide sequences with keeping alignment gaps by using an in-house perl script (see *SUPPLEMENTARY CODE*). Using another in-house perl script (see *SUPPLEMENTARY CODE*), synonymous and nonsynonymous nucleotide divergence per site between all pairs of sequences were computed based on the modified Nei-Gojobori method (Zhang et al. 1998) with complete deletion option

and Ti/Tv (transition-transversion ratio) = 2. Finally, synonymous and nonsynonymous nucleotide distances on each branch were computed by the least-squares method (Rzhetsky and Nei 1993).

Estimation of parallel pseudogenization on neo-sex chromosomes

In *D. miranda* and *D. albomicans*, the Muller element C independently became neo-sex chromosomes. The number of parallel pseudogenization in these two lineages was therefore examined. First, all orthologs that are located on the same Muller elements during the evolution of the three species considered, do not have any inparalogs, and functional in the outgroup species (*D. obscura* for *D. miranda* and *D. kohkoa* for *D. albomicans*) were collected. To identify the orthologs among the six species (i.e., *D. miranda*, *D. pseudoobscura*, *D. obscura*, *D. albomicans*, *D. nasuta*, and *D. kohkoa*), reciprocal homology search based on BLASTP ver. 2.9.0+ was conducted between the outgroup species of each trio (i.e., *D. obscura* and *D. kohkoa*) with a cut-off e-value of 10^{-10}. Then, we identified orthologs that show reciprocal best-hit relationship between the species, located on the same Muller elements, and do not have any inparalogs. Finally, the information of orthologous genes for each trio species was added to the orthologs identified in *D. obscura* and *D. kohkoa*. If the pseudogenization for an ortholog was inferred on the same lineages in the two trios (e.g., the neo-Y lineages in *D. miranda* and *D. albomicans*), the ortholog was regarded to have experienced parallel pseudogenization.

To evaluate whether the observed number of parallel pseudogenization events has some biological meaning, we conducted a binomial test. As an example, let us think about Muller element A in *D. miranda* and *D. albomicans* (Fig. 6SA). There were 29 and 38 pseudogenizations in the *D. miranda* and the *D. albomicans* lineages, respectively. Since the number of orthologs analyzed was 678, the expected probability that the same gene is independently pseudogenized in both lineages is (29/678) × (38/678) = 0.0024. With this expected probability, the cumulative probability in which the number of

shared pseudogenizations among 678 orthologs exceeds the observed number of shared pseudogenizations (i.e., five in this example) was computed by a binomial test. In this example, the cumulative probability (i.e., *P*-value) was 0.025. However, correction of multiple testing finally gave the *Q*-value of 0.074, i.e., an insignificant value.

Gene Ontology analysis

To examine Gene Ontology that are enriched in the functional and nonfunctional genes on neo-sex chromosomes, using the neo-sex-linked genes as queries, we conducted a homology search against the amino-acid sequences in *D. melanogaster* [dmel-all-translation-r6.34.fasta from FlyBase (https://flybase.org/)] based on BLASTP ver. 2.9.0+ with a cut-off e-value of 10^{-10}. The best-hit gene in *D. melanogaster* was then used for the Gene Ontology analysis by using the GOrilla software (Eden et al. 2009).

Table S1. Summary of the DNA sequencing data of the *Drosophila* species used in this study.

Species	Sex	Sample name	Platform	Layout/length (bp)	Accession	Reference
D. miranda	Female	mirF	HiSeq 2000	Paired/101	DRR055276	Nozawa et al. (2016)
	Male	mirM	HiSeq 2000	Paired/101	DRR055277	Nozawa et al. (2016)
D. albomicans	Female	albF	PacBio RS II	Single/-	DRR075970-99	This study
			HiSeq 2500	Paired/500	DRR076000	This study
	Male	albM	HiSeq 2500	Paired/500	DRR076001	This study
D. nasuta	Female	nasF	PacBio RS II	Single/-	DRR125226	This study
			HiSeq 2500	Paired/400	DRR061014	This study
D. kohkoa	Female	kohF	PacBio Sequel	Single/-	DRR160727-33	This study
			HiSeq 2500	Paired/500	DRR160734	This study
D. americana	Female	ameF	PacBio RS II	Single/-	DRR076002-26	This study
			HiSeq 2500	Paired/500	DRR076027	This study
	Male	ameM	HiSeq 2500	Paired/500	DRR076028	This study
D. texana	Female	texF	PacBio Sequel	Single/-	DRR160721-4	This study
			HiSeq 2500	Paired/500	DRR160725	This study
D. novamexicana	Female	novF	PacBio Sequel	Single/-	DRR160735-9	This study
			HiSeq 2500	Paired/500	DRR160740	This study

Table S2. Assembly size, number of contigs, and contig N50 of the *Drosophila* genomes used in this study.

Species	Chrs. included	Assembly size (bp)	No. of contigs	Contig N50 (bp)	Accession	Reference
D. miranda[1]	w/o Y/neo-Y	176,610,581	40	32,547,436[2]	-	Mahajan et al. (2018)
	with Y/neo-Y	287,124,465	102	35,279,367	QNQS01000001-01000102	Mahajan et al. (2018)
D. pseudoobscura	w/o Y	152,696,384	4,790	12,541,198	AADE01000001-01017507	Richards et al. (2005)
D. obscura	w/o Y	181,868,570	1,935	472,512[2]	BDQP01000001-01001935	Nozawa et al. (2016)
D. albomicans	w/o Y/neo-Y	182,697,126	834	21,972,321	BJEI01000001-01000834	This study
	with neo-Y	238,238,472	836	25,367,705	-	This study
D. nasuta	w/o Y	173,158,203	604	17,893,789	BJEH01000001-01000604	This study
D. kohkoa	w/o Y	170,668,061	87	3,597,765	BJEL01000001-01000087	This study
D. americana	w/o Y/neo-Y	177,534,117	435	1,565,372	BJEJ01000001-01000435	This study
	with neo-Y	207,397,045	453	1,605,128	-	This study
D. texana	w/o Y	165,405,863	199	2,693,102	BJEK01000001-01000199	This study
D. novamexicana	w/o Y	173,633,261	270	2,873,990	BJEM01000001-01000270	This study

[1] Data are based on the resequence in this study.

[2] Based on scaffolds but not contigs.

Table S3. Assessment of genome assembly of the nine *Drosophila* species used in this study based on the existence of BUSCOs.

Assembly	Number (proportion) of genes				
	Complete SC[1]	Complete D[2]	Fragmented	Missing	Total
D. miranda	3,180 (96.8%)	78 (2.4%)	6 (0.2%)	21 (0.6%)	3,285 (100%)
D. miranda with Y/neo-Y	2,765 (84.2%)	493 (15.0%)	6 (0.2%)	21 (0.6%)	3,285 (100%)
D. pseudoobscura	3,167 (96.4%)	54 (1.6%)	17 (0.5%)	47 (1.4%)	3,285 (100%)
D. obscura	3,100 (94.4%)	153 (4.7%)	11 (0.3%)	21 (0.6%)	3,285 (100%)
D. albomicans	3,202 (97.5%)	56 (1.7%)	5 (0.2%)	22 (0.7%)	3,285 (100%)
D. albomicans with neo-Y	1,934 (58.9%)	1,324 (40.3%)	5 (0.2%)	22 (0.7%)	3,285 (100%)
D. nasuta	3,230 (98.3%)	29 (0.9%)	6 (0.2%)	20 (0.6%)	3,285 (100%)
D. kohkoa	3,042 (92.6%)	210 (6.4%)	8 (0.2%)	25 (0.8%)	3,285 (100%)
D. americana	3,116 (94.9%)	103 (3.1%)	21 (0.6%)	45 (1.4%)	3,285 (100%)
D. americana with neo-Y	2,544 (77.4%)	678 (20.6%)	19 (0.6%)	44 (1.3%)	3,285 (100%)
D. texana	3,202 (97.5%)	51 (1.6%)	7 (0.2%)	25 (0.8%)	3,285 (100%)
D. novamexicana	3,156 (96.1%)	99 (3.0%)	7 (0.2%)	23 (0.7%)	3,285 (100%)

BUSCO ver. 4.0.4 software (Seppey et al. 2019) was used with the "diptera_odb10" dataset.

[1] Single copy genes.

[2] Duplicated genes. It should be mentioned that when contigs/scaffolds from neo-Y is included in the analysis, the proportion of complete duplicated ORFs considerably increases, because the homologs on neo-X and neo-Y were regarded as duplicated genes.

Table S4. Summary of the RNA sequencing data of the *Drosophila* species used in this study.

Species	Sex	Tissue	Sample name	Platform	Layout/length (nt)	Accession[1]	Reference
D. miranda	Female	Larval whole body	mirLF	HiSeq 2000	Paired/101	DRR055176, DRR055177	Nozawa et al. (2016)
	Male		mirLM	HiSeq 2000	Paired/101	DRR055178, DRR055179	Nozawa et al. (2016)
	Female	Pupal whole body	mirPF	HiSeq 2000	Paired/101	DRR055186, DRR055187	Nozawa et al. (2016)
	Male		mirPM	HiSeq 2000	Paired/101	DRR055188, DRR055189	Nozawa et al. (2016)
	Female	Adult whole body	mirWF	HiSeq 2000	Paired/101	DRR055196, DRR055197	Nozawa et al. (2016)
	Male		mirWM	HiSeq 2000	Paired/101	DRR055198, DRR055199	Nozawa et al. (2016)
	Female	Ovary	mirO	HiSeq 2000	Paired/101	DRR055184, DRR055185	Nozawa et al. (2016)
	Male	Testis	mirTe	HiSeq 2000	Paired/101	DRR055194, DRR055195	Nozawa et al. (2016)
D. pseudoobscura	Female	Larval whole body	pseLF	HiSeq 2000	Paired/100	DRR055252, DRR055253	Nozawa et al. (2016)
	Male		pseLM	HiSeq 2000	Paired/100	DRR055254, DRR055255	Nozawa et al. (2016)
	Female	Pupal whole body	psePF	HiSeq 2000	Paired/100	DRR055262, DRR055263	Nozawa et al. (2016)
	Male		psePM	HiSeq 2000	Paired/100	DRR055264, DRR055265	Nozawa et al. (2016)
	Female	Adult whole body	pseWF	HiSeq 2000	Paired/101	DRR055272, DRR055273	Nozawa et al. (2016)
	Male		pseWM	HiSeq 2000	Paired/101	DRR055274, DRR055275	Nozawa et al. (2016)
	Female	Ovary	pseO	HiSeq 2000	Paired/101	DRR055260, DRR055261	Nozawa et al. (2016)
	Male	Testis	pseTe	HiSeq 2000	Paired/101	DRR055270, DRR055271	Nozawa et al. (2016)
D. obscura	Female	Larval whole body	obsLF	HiSeq 2000	Paired/101	DRR055214, DRR055215	Nozawa et al. (2016)
	Male		obsLM	HiSeq 2000	Paired/101	DRR055216, DRR055217	Nozawa et al. (2016)
	Female	Pupal whole body	obsPF	HiSeq 2000	Paired/101	DRR055218, DRR055219	Nozawa et al. (2016)
	Male		obsPM	HiSeq 2000	Paired/101	DRR055220, DRR055221	Nozawa et al. (2016)
	Female	Adult whole body	obsWF	HiSeq 2000	Paired/101	DRR055230, DRR055231	Nozawa et al. (2016)
	Male		obsWM	HiSeq 2000	Paired/101	DRR055232, DRR055233	Nozawa et al. (2016)
	Female	Ovary	obsO	HiSeq 2000	Paired/101	DRR055218, DRR055219	Nozawa et al. (2016)
	Male	Testis	obsTe	HiSeq 2000	Paired/101	DRR055228, DRR055229	Nozawa et al. (2016)

Table S4. Cont'd.

Species	Sex	Tissue	Sample name	Platform	Layout/length (nt)	Accession[1]	Reference
D. albomicans	Female	Larval whole body	albLF	HiSeq 4000	Paired/101	DRR160743	This study
	Male		albLM	HiSeq 4000	Paired/101	DRR160744	This study
	Female	Pupal whole body	albPF	HiSeq 4000	Paired/101	DRR160745	This study
	Male		albPM	HiSeq 4000	Paired/101	DRR160746	This study
	Female	Adult whole body	albWF	HiSeq 4000	Paired/101	DRR160741	This study
	Male		albWM	HiSeq 4000	Paired/101	DRR160742	This study
	Female	Ovary	albO	HiSeq 4000	Paired/101	DRR160747	This study
	Male	Testis	albTe	HiSeq 4000	Paired/101	DRR160748	This study
D. nasuta	Female	Larval whole body	nasLF	HiSeq 4000	Paired/101	DRR160751	This study
	Male		nasLM	HiSeq 4000	Paired/101	DRR160752	This study
	Female	Pupal whole body	nasPF	HiSeq 4000	Paired/101	DRR160753	This study
	Male		nasPM	HiSeq 4000	Paired/101	DRR160754	This study
	Female	Adult whole body	nasWF	HiSeq 4000	Paired/101	DRR160749	This study
	Male		nasWM	HiSeq 4000	Paired/101	DRR160750	This study
	Female	Ovary	nasO	HiSeq 4000	Paired/101	DRR160755	This study
	Male	Testis	nasTe	HiSeq 4000	Paired/101	DRR160756	This study
D. kohkoa	Female	Larval whole body	kohLF	HiSeq 4000	Paired/101	DRR160759	This study
	Male		kohLM	HiSeq 4000	Paired/101	DRR160760	This study
	Female	Pupal whole body	kohPF	HiSeq 4000	Paired/101	DRR160761	This study
	Male		kohPM	HiSeq 4000	Paired/101	DRR160762	This study
	Female	Adult whole body	kohWF	HiSeq 4000	Paired/101	DRR160757	This study
	Male		kohWM	HiSeq 4000	Paired/101	DRR160758	This study
	Female	Ovary	kohO	HiSeq X	Paired/151	DRR168781	This study
	Male	Testis	kohTe	HiSeq X	Paired/151	DRR168782	This study

Table S4. Cont'd.

Species	Sex	Tissue	Sample name	Platform	Layout/length (nt)	Accession[1]	Reference
D. americana	Female	Larval whole	ameLF	HiSeq 4000	Paired/101	DRR160779	This study
	Male		ameLM	HiSeq 4000	Paired/101	DRR160780	This study
	Female	Pupal whole body	amePF	HiSeq 4000	Paired/101	DRR160781	This study
	Male		amePM	HiSeq 4000	Paired/101	DRR160782	This study
	Female	Adult whole body	ameWF	HiSeq 4000	Paired/101	DRR160777	This study
	Male		ameWM	HiSeq 4000	Paired/101	DRR160778	This study
	Female	Ovary	ameO	HiSeq 4000	Paired/101	DRR160783	This study
	Male	Testis	ameTe	HiSeq 4000	Paired/101	DRR160784	This study
D. texana	Female	Larval whole	texLF	HiSeq 4000	Paired/101	DRR160771	This study
	Male		texLM	HiSeq 4000	Paired/101	DRR160772	This study
	Female	Pupal whole body	texPF	HiSeq 4000	Paired/101	DRR160773	This study
	Male		texPM	HiSeq 4000	Paired/101	DRR160774	This study
	Female	Adult whole body	texWF	HiSeq 4000	Paired/101	DRR160769	This study
	Male		texWM	HiSeq 4000	Paired/101	DRR160770	This study
	Female	Ovary	texO	HiSeq 4000	Paired/101	DRR160775	This study
	Male	Testis	texTe	HiSeq 4000	Paired/101	DRR160776	This study
D. novamexicana	Female	Larval whole	novLF	HiSeq 4000	Paired/101	DRR160765	This study
	Male		novLM	HiSeq 4000	Paired/101	DRR160766	This study
	Female	Pupal whole body	novPF	HiSeq 4000	Paired/101	DRR160767	This study
	Male		novPM	HiSeq 4000	Paired/101	DRR160768	This study
	Female	Adult whole body	novWF	HiSeq 4000	Paired/101	DRR160763	This study
	Male		novWM	HiSeq 4000	Paired/101	DRR160764	This study
	Female	Ovary	novO	HiSeq X	Paired/151	DRR168783	This study
	Male	Testis	novTe	HiSeq X	Paired/151	DRR168784	This study

[1] Each accession number newly deposited in this study contains run data for two biological replicates.

Table S5. Numbers of protein-coding genes and their transcripts of the *Drosophila* species used in this study.

Species	No. of functional protein-coding genes	No. of transcripts from functional protein-coding genes	No. of non-functional protein-coding genes[2]
D. miranda	11,299 (13,161)[1]	24,541 (28,773)	4,698 (12,167)
D. pseudoobscura	10,800	19,929	3,733
D. obscura	11,330	21,332	4,809
D. albomicans	10,101 (13,834)	19,880 (26,172)	3,659 (4,685)
D. nasuta	9,868	19,196	3,280
D. kohkoa	10,183	19,865	3,176
D. americana	9,615 (11,403)	20,064 (22,916)	3,364 (3,860)
D. texana	9,910	19,770	2,692
D. novamexicana	9,722	20,400	2,940

[1] Numbers in parentheses include the counts of Y/neo-Y-linked genes/transcripts.

[2] Unclassified genes are included in the counts.

Table S8. Enriched GO terms in functional genes on the neo-X in *Drosophila miranda*.

GO term	Description	*P*-value[1]	FDR *Q*-value	Enrichment	Category
GO:0044237	cellular metabolic process	4.12E-05	1.86E-01	1.05	Process
GO:0009987	cellular process	3.74E-04	8.42E-01	1.03	Process
GO:0008152	metabolic process	1.00E-03	1.00E+00	1.03	Process
GO:0003824	catalytic activity	2.12E-04	2.73E-01	1.05	Function
GO:0044424	intracellular part	1.95E-06	1.61E-03	1.04	Component
GO:0044422	organelle part	1.26E-05	5.20E-03	1.06	Component
GO:0044446	intracellular organelle part	2.62E-05	7.24E-03	1.06	Component
GO:0044444	cytoplasmic part	2.85E-05	5.90E-03	1.06	Component
GO:0032991	protein-containing complex	1.06E-04	1.76E-02	1.06	Component
GO:0005739	mitochondrion	5.93E-04	8.18E-02	1.11	Component

[1] Only GO terms with *P*-value ≤ 0.001 are listed.

Table S9. Enriched GO terms in functional genes on the neo-X in *Drosophila albomicans*.

GO term	Description	*P*-value[1]	FDR *Q*-value	Enrichment	Category
GO:0008152	metabolic process	2.21E-10	1.23E-06	1.05	Process
GO:0071704	organic substance metabolic process	1.22E-08	3.39E-05	1.05	Process
GO:0044237	cellular metabolic process	1.85E-08	3.42E-05	1.05	Process
GO:0044238	primary metabolic process	9.46E-08	1.32E-04	1.05	Process
GO:0006807	nitrogen compound metabolic process	2.05E-06	2.28E-03	1.05	Process
GO:0043170	macromolecule metabolic process	1.41E-05	1.31E-02	1.05	Process
GO:1901564	organonitrogen compound metabolic process	3.51E-05	2.79E-02	1.05	Process
GO:0009987	cellular process	6.97E-05	4.84E-02	1.02	Process
GO:0044281	small molecule metabolic process	8.70E-05	5.37E-02	1.09	Process
GO:0009058	biosynthetic process	1.14E-04	6.36E-02	1.08	Process
GO:0006629	lipid metabolic process	1.43E-04	7.20E-02	1.11	Process
GO:0043603	cellular amide metabolic process	1.56E-04	7.21E-02	1.13	Process
GO:1901576	organic substance biosynthetic process	1.89E-04	8.07E-02	1.07	Process
GO:0032787	monocarboxylic acid metabolic process	2.49E-04	9.89E-02	1.16	Process
GO:0034660	ncRNA metabolic process	2.70E-04	9.99E-02	1.12	Process
GO:0043436	oxoacid metabolic process	2.79E-04	9.70E-02	1.11	Process
GO:0006082	organic acid metabolic process	2.79E-04	9.13E-02	1.11	Process
GO:0044255	cellular lipid metabolic process	2.98E-04	9.19E-02	1.11	Process
GO:0044249	cellular biosynthetic process	3.28E-04	9.60E-02	1.07	Process
GO:0043604	amide biosynthetic process	3.65E-04	1.01E-01	1.14	Process

Table S9. Cont'd.

GO term	Description	*P*-value[1]	FDR *Q*-value	Enrichment	Category
GO:0019752	carboxylic acid metabolic process	5.40E-04	1.43E-01	1.11	Process
GO:0034470	ncRNA processing	7.14E-04	1.80E-01	1.13	Process
GO:0009056	catabolic process	7.22E-04	1.74E-01	1.07	Process
GO:0006399	tRNA metabolic process	7.22E-04	1.67E-01	1.16	Process
GO:0034641	cellular nitrogen compound metabolic process	7.42E-04	1.65E-01	1.05	Process
GO:1901575	organic substance catabolic process	8.85E-04	1.89E-01	1.07	Process
GO:0034645	cellular macromolecule biosynthetic process	9.07E-04	1.87E-01	1.10	Process
GO:0003824	catalytic activity	3.60E-09	6.49E-06	1.06	Function
GO:0017111	nucleoside-triphosphatase activity	4.69E-06	4.23E-03	1.13	Function
GO:0016817	hydrolase activity, acting on acid anhydrides	1.09E-05	6.55E-03	1.13	Function
GO:0016818	hydrolase activity, acting on acid anhydrides, in phosphorus-containing anhydrides	1.09E-05	4.91E-03	1.13	Function
GO:0016462	pyrophosphatase activity	1.24E-05	4.46E-03	1.13	Function
GO:0016787	hydrolase activity	1.97E-05	5.93E-03	1.07	Function
GO:0043168	anion binding	1.30E-04	3.36E-02	1.07	Function
GO:0036094	small molecule binding	4.67E-04	1.05E-01	1.07	Function
GO:0043167	ion binding	5.59E-04	1.12E-01	1.05	Function
GO:0003735	structural constituent of ribosome	7.22E-04	1.30E-01	1.16	Function
GO:1901265	nucleoside phosphate binding	8.54E-04	1.40E-01	1.07	Function
GO:0000166	nucleotide binding	8.54E-04	1.28E-01	1.07	Function
GO:0019001	guanyl nucleotide binding	9.78E-04	1.36E-01	1.16	Function

Table S9. Cont'd.

GO term	Description	*P*-value[1]	FDR *Q*-value	Enrichment	Category
GO:0044424	intracellular part	3.53E-10	3.60E-07	1.04	Component
GO:0044444	cytoplasmic part	4.24E-07	2.16E-04	1.05	Component
GO:0044464	cell part	4.94E-06	1.68E-03	1.02	Component
GO:0032991	protein-containing complex	8.28E-05	2.11E-02	1.05	Component
GO:0005737	cytoplasm	1.95E-04	3.97E-02	1.05	Component
GO:1902494	catalytic complex	3.48E-04	5.91E-02	1.07	Component
GO:0044391	ribosomal subunit	5.33E-04	7.76E-02	1.16	Component
GO:0098588	bounding membrane of organelle	5.54E-04	7.05E-02	1.14	Component
GO:0098805	whole membrane	7.22E-04	8.18E-02	1.16	Component
GO:0005739	mitochondrion	9.18E-04	9.35E-02	1.09	Component

[1] Only GO terms with *P*-value ≤ 0.001 are listed.

Table S10. Enriched GO terms in functional genes on the neo-X in *Drosophila americana*.

GO term	Description	*P*-value[1]	FDR *Q*-value	Enrichment	Category
GO:0044237	cellular metabolic process	8.28E-06	3.72E-02	1.06	Process
GO:0006807	nitrogen compound metabolic process	1.44E-05	3.24E-02	1.06	Process
GO:0008152	metabolic process	3.43E-05	5.14E-02	1.05	Process
GO:0044238	primary metabolic process	1.68E-04	1.89E-01	1.05	Process
GO:0043170	macromolecule metabolic process	2.21E-04	1.98E-01	1.06	Process
GO:0071704	organic substance metabolic process	2.72E-04	2.04E-01	1.05	Process
GO:0044260	cellular macromolecule metabolic process	3.87E-04	2.49E-01	1.07	Process
GO:1901360	organic cyclic compound metabolic process	4.92E-04	2.77E-01	1.08	Process
GO:0006725	cellular aromatic compound metabolic process	5.91E-04	2.95E-01	1.08	Process
GO:0034641	cellular nitrogen compound metabolic process	6.06E-04	2.73E-01	1.07	Process
GO:1901564	organonitrogen compound metabolic process	9.14E-04	3.73E-01	1.06	Process
GO:0003824	catalytic activity	1.43E-04	1.83E-01	1.05	Function

[1] Only GO terms with *P*-value ≤ 0.001 are listed.

Table S11. Enriched GO terms in pseudogenes on the neo-X in *Drosophila miranda*.

GO term	Description	*P*-value[1]	FDR *Q*-value	Enrichment	Category
GO:0009593	detection of chemical stimulus	7.68E-18	3.46E-14	6.29	Process
GO:0051606	detection of stimulus	5.08E-12	1.14E-08	4.40	Process
GO:0050907	detection of chemical stimulus involved in sensory perception	3.73E-10	5.60E-07	6.77	Process
GO:0050911	detection of chemical stimulus involved in sensory perception of smell	2.63E-09	2.96E-06	6.72	Process
GO:0050906	detection of stimulus involved in sensory perception	1.92E-08	1.73E-05	5.30	Process
GO:0007606	sensory perception of chemical stimulus	8.17E-06	6.13E-03	3.04	Process
GO:0007600	sensory perception	2.89E-05	1.86E-02	2.63	Process
GO:0050877	nervous system process	7.04E-05	3.96E-02	2.30	Process
GO:0050909	sensory perception of taste	3.56E-04	1.78E-01	4.89	Process
GO:0038023	signaling receptor activity	2.93E-13	3.77E-10	4.00	Function
GO:0004888	transmembrane signaling receptor activity	1.86E-12	1.20E-09	4.12	Function
GO:0060089	molecular transducer activity	1.89E-12	8.10E-10	3.79	Function
GO:0004984	olfactory receptor activity	2.63E-09	8.47E-07	6.72	Function
GO:0005549	odorant binding	2.08E-06	5.37E-04	3.80	Function
GO:0008527	taste receptor activity	6.10E-06	1.31E-03	7.33	Function
GO:0022834	ligand-gated channel activity	7.07E-06	1.30E-03	4.58	Function
GO:0015276	ligand-gated ion channel activity	7.07E-06	1.14E-03	4.58	Function
GO:0022839	ion gated channel activity	2.32E-05	3.32E-03	3.40	Function
GO:0022836	gated channel activity	2.32E-05	2.99E-03	3.40	Function
GO:0004930	G protein-coupled receptor activity	3.25E-05	3.80E-03	4.89	Function

Table S11. Cont'd.

GO term	Description	*P*-value[1]	FDR *Q*-value	Enrichment	Category
GO:0005216	ion channel activity	3.94E-05	4.22E-03	3.11	Function
GO:0022838	substrate-specific channel activity	8.63E-05	8.55E-03	2.93	Function
GO:0022803	passive transmembrane transporter activity	3.36E-04	3.09E-02	2.63	Function
GO:0015267	channel activity	3.36E-04	2.88E-02	2.63	Function
GO:0032590	dendrite membrane	2.63E-09	2.18E-06	6.72	Component
GO:0032589	neuron projection membrane	2.04E-07	8.44E-05	5.38	Component
GO:0031256	leading edge membrane	2.04E-07	5.63E-05	5.38	Component
GO:0031253	cell projection membrane	1.43E-06	2.96E-04	4.75	Component
GO:0016021	integral component of membrane	2.22E-04	3.68E-02	1.61	Component
GO:0031224	intrinsic component of membrane	2.50E-04	3.45E-02	1.60	Component
GO:0120038	plasma membrane bounded cell projection part	4.13E-04	4.89E-02	2.07	Component
GO:0044463	cell projection part	4.13E-04	4.28E-02	2.07	Component

[1] Only GO terms with *P*-value ≤ 0.001 are listed.

Table S12. Enriched GO terms in pseudogenes on the neo-X in *Drosophila albomicans*.

GO term	Description	*P*-value[1]	FDR *Q*-value	Enrichment	Category
GO:0009593	detection of chemical stimulus	1.33E-17	7.38E-14	5.17	Process
GO:0051606	detection of stimulus	1.31E-12	3.65E-09	3.58	Process
GO:0050906	detection of stimulus involved in sensory perception	9.53E-12	1.77E-08	4.45	Process
GO:0050907	detection of chemical stimulus involved in sensory perception	1.35E-11	1.87E-08	5.13	Process
GO:0050911	detection of chemical stimulus involved in sensory perception of smell	7.61E-11	8.46E-08	5.85	Process
GO:0007606	sensory perception of chemical stimulus	6.63E-06	6.14E-03	2.60	Process
GO:0007600	sensory perception	7.60E-05	6.03E-02	2.12	Process
GO:0050877	nervous system process	8.96E-05	6.23E-02	1.85	Process
GO:0006355	regulation of transcription, DNA-templated	9.31E-04	5.75E-01	1.38	Process
GO:2001141	regulation of RNA biosynthetic process	9.31E-04	5.17E-01	1.38	Process
GO:1903506	regulation of nucleic acid-templated transcription	9.31E-04	4.70E-01	1.38	Process
GO:0004984	olfactory receptor activity	5.20E-10	9.37E-07	5.49	Function
GO:0038023	signaling receptor activity	1.96E-08	1.76E-05	2.39	Function
GO:0060089	molecular transducer activity	1.58E-07	9.49E-05	2.24	Function
GO:0005216	ion channel activity	1.86E-07	8.40E-05	2.85	Function
GO:0022839	ion gated channel activity	2.45E-07	8.85E-05	3.14	Function
GO:0022836	gated channel activity	2.45E-07	7.37E-05	3.14	Function
GO:0005549	odorant binding	3.43E-07	8.83E-05	3.55	Function
GO:0004888	transmembrane signaling receptor activity	4.05E-07	9.12E-05	2.38	Function
GO:0022838	substrate-specific channel activity	4.36E-07	8.74E-05	2.75	Function

Table S12. Cont'd.

GO term	Description	*P*-value[1]	FDR *Q*-value	Enrichment	Category
GO:0022834	ligand-gated channel activity	1.27E-06	2.28E-04	3.62	Function
GO:0015276	ligand-gated ion channel activity	1.27E-06	2.07E-04	3.62	Function
GO:0022803	passive transmembrane transporter activity	2.92E-06	4.39E-04	2.53	Function
GO:0015267	channel activity	2.92E-06	4.06E-04	2.53	Function
GO:0003700	DNA-binding transcription factor activity	3.35E-05	4.31E-03	1.81	Function
GO:0005261	cation channel activity	8.69E-05	1.04E-02	2.77	Function
GO:0000981	DNA-binding transcription factor activity, RNA polymerase II-specific	1.16E-04	1.30E-02	1.81	Function
GO:0140110	transcription regulator activity	1.50E-04	1.59E-02	1.62	Function
GO:0000977	RNA polymerase II regulatory region sequence-specific DNA binding	1.55E-04	1.56E-02	1.81	Function
GO:0001012	RNA polymerase II regulatory region DNA binding	1.55E-04	1.48E-02	1.81	Function
GO:0003690	double-stranded DNA binding	1.78E-04	1.60E-02	1.70	Function
GO:0000976	transcription regulatory region sequence-specific DNA binding	1.82E-04	1.56E-02	1.75	Function
GO:0044212	transcription regulatory region DNA binding	1.82E-04	1.49E-02	1.75	Function
GO:1990837	sequence-specific double-stranded DNA binding	1.96E-04	1.53E-02	1.71	Function
GO:0001067	regulatory region nucleic acid binding	2.14E-04	1.61E-02	1.73	Function
GO:0043565	sequence-specific DNA binding	3.32E-04	2.39E-02	1.63	Function
GO:0003677	DNA binding	3.82E-04	2.65E-02	1.48	Function
GO:0008527	taste receptor activity	8.72E-04	5.82E-02	4.18	Function
GO:0032590	dendrite membrane	1.62E-08	1.65E-05	5.38	Component

Table S12. Cont'd.

GO term	Description	*P*-value[1]	FDR *Q*-value	Enrichment	Category
GO:0032589	neuron projection membrane	8.96E-08	4.57E-05	4.39	Component
GO:0031256	leading edge membrane	8.96E-08	3.04E-05	4.39	Component
GO:0031253	cell projection membrane	2.93E-07	7.47E-05	3.92	Component
GO:0071683	sensory dendrite	1.60E-05	3.27E-03	6.27	Component
GO:0097458	neuron part	1.37E-04	2.33E-02	1.69	Component
GO:0120038	plasma membrane bounded cell projection part	2.21E-04	3.21E-02	1.78	Component
GO:0044463	cell projection part	2.21E-04	2.81E-02	1.78	Component
GO:0098590	plasma membrane region	3.42E-04	3.87E-02	1.92	Component
GO:0030425	dendrite	9.99E-04	1.02E-01	2.37	Component

[1] Only GO terms with *P*-value ≤ 0.001 are listed.

Table S13. Enriched GO terms in pseudogenes on the neo-X in *Drosophila americana*.

GO term	Description	*P*-value[1]	FDR *Q*-value	Enrichment	Category
GO:0050907	detection of chemical stimulus involved in sensory perception	4.75E-05	2.13E-01	5.12	Process
GO:0009593	detection of chemical stimulus	4.75E-05	1.07E-01	5.12	Process
GO:0050906	detection of stimulus involved in sensory perception	1.65E-04	2.47E-01	4.05	Process
GO:0050911	detection of chemical stimulus involved in sensory perception of smell	2.50E-04	2.80E-01	4.93	Process
GO:0004984	olfactory receptor activity	2.50E-04	3.18E-01	4.93	Function
GO:0005549	odorant binding	3.30E-04	2.11E-01	4.19	Function
GO:0038023	signaling receptor activity	8.90E-04	3.79E-01	2.24	Function
GO:0043565	sequence-specific DNA binding	9.76E-04	3.11E-01	1.82	Function
GO:0032590	dendrite membrane	6.54E-04	5.31E-01	4.38	Component

[1] Only GO terms with *P*-value ≤ 0.001 are listed.

Table S14. Enriched GO terms in functional genes on the neo-Y in *Drosophila miranda*.

GO term	Description	*P*-value[1]	FDR *Q*-value	Enrichment	Category
GO:0048523	negative regulation of cellular process	3.93E-07	1.75E-03	1.25	Process
GO:0045184	establishment of protein localization	1.21E-06	2.69E-03	1.43	Process
GO:0009987	cellular process	1.21E-06	1.80E-03	1.07	Process
GO:0051171	regulation of nitrogen compound metabolic process	1.31E-06	1.46E-03	1.18	Process
GO:0080090	regulation of primary metabolic process	1.63E-06	1.45E-03	1.18	Process
GO:0031323	regulation of cellular metabolic process	1.66E-06	1.23E-03	1.17	Process
GO:0046907	intracellular transport	1.82E-06	1.16E-03	1.36	Process
GO:0009653	anatomical structure morphogenesis	3.10E-06	1.72E-03	1.27	Process
GO:0015031	protein transport	3.37E-06	1.66E-03	1.43	Process
GO:0050794	regulation of cellular process	3.80E-06	1.69E-03	1.12	Process
GO:0032502	developmental process	6.60E-06	2.67E-03	1.16	Process
GO:0016043	cellular component organization	6.60E-06	2.45E-03	1.16	Process
GO:0048519	negative regulation of biological process	6.87E-06	2.35E-03	1.20	Process
GO:0042886	amide transport	7.74E-06	2.46E-03	1.41	Process
GO:0071840	cellular component organization or biogenesis	7.94E-06	2.36E-03	1.16	Process
GO:0033036	macromolecule localization	1.09E-05	3.02E-03	1.29	Process
GO:0015833	peptide transport	1.11E-05	2.92E-03	1.41	Process
GO:0008104	protein localization	1.24E-05	3.05E-03	1.31	Process
GO:0060255	regulation of macromolecule metabolic process	1.75E-05	4.10E-03	1.15	Process
GO:0019222	regulation of metabolic process	1.85E-05	4.12E-03	1.15	Process

Table S14. Cont'd.

GO term	Description	*P*-value[1]	FDR *Q*-value	Enrichment	Category
GO:0048518	positive regulation of biological process	2.28E-05	4.84E-03	1.17	Process
GO:0048522	positive regulation of cellular process	2.64E-05	5.34E-03	1.18	Process
GO:0044237	cellular metabolic process	3.49E-05	6.74E-03	1.10	Process
GO:0006886	intracellular protein transport	4.23E-05	7.84E-03	1.43	Process
GO:0051649	establishment of localization in cell	6.40E-05	1.14E-02	1.27	Process
GO:0010646	regulation of cell communication	8.03E-05	1.37E-02	1.24	Process
GO:0023051	regulation of signaling	8.03E-05	1.32E-02	1.24	Process
GO:0051641	cellular localization	8.99E-05	1.43E-02	1.24	Process
GO:0050789	regulation of biological process	9.41E-05	1.44E-02	1.09	Process
GO:0003006	developmental process involved in reproduction	1.30E-04	1.93E-02	1.25	Process
GO:0048585	negative regulation of response to stimulus	1.37E-04	1.97E-02	1.31	Process
GO:0010604	positive regulation of macromolecule metabolic process	1.44E-04	2.00E-02	1.22	Process
GO:0002181	cytoplasmic translation	1.95E-04	2.63E-02	1.60	Process
GO:0006412	translation	2.21E-04	2.88E-02	1.46	Process
GO:0043043	peptide biosynthetic process	2.21E-04	2.80E-02	1.46	Process
GO:0010468	regulation of gene expression	2.23E-04	2.75E-02	1.16	Process
GO:0022414	reproductive process	2.98E-04	3.58E-02	1.18	Process
GO:0051252	regulation of RNA metabolic process	3.02E-04	3.53E-02	1.18	Process
GO:0044260	cellular macromolecule metabolic process	3.02E-04	3.45E-02	1.13	Process
GO:0065007	biological regulation	3.13E-04	3.48E-02	1.08	Process

Table S14. Cont'd.

GO term	Description	*P*-value[1]	FDR *Q*-value	Enrichment	Category
GO:0031324	negative regulation of cellular metabolic process	3.57E-04	3.87E-02	1.25	Process
GO:0051246	regulation of protein metabolic process	3.75E-04	3.97E-02	1.24	Process
GO:0048583	regulation of response to stimulus	3.90E-04	4.03E-02	1.19	Process
GO:0048869	cellular developmental process	3.98E-04	4.02E-02	1.19	Process
GO:0023057	negative regulation of signaling	4.26E-04	4.21E-02	1.31	Process
GO:2000112	regulation of cellular macromolecule biosynthetic process	4.62E-04	4.47E-02	1.16	Process
GO:0051172	negative regulation of nitrogen compound metabolic process	4.98E-04	4.72E-02	1.26	Process
GO:0022412	cellular process involved in reproduction in multicellular organism	5.33E-04	4.93E-02	1.23	Process
GO:0010648	negative regulation of cell communication	5.70E-04	5.17E-02	1.31	Process
GO:1901566	organonitrogen compound biosynthetic process	5.75E-04	5.11E-02	1.29	Process
GO:0009966	regulation of signal transduction	6.14E-04	5.35E-02	1.21	Process
GO:0010556	regulation of macromolecule biosynthetic process	6.68E-04	5.71E-02	1.16	Process
GO:0071705	nitrogen compound transport	6.92E-04	5.81E-02	1.26	Process
GO:0032268	regulation of cellular protein metabolic process	7.17E-04	5.91E-02	1.23	Process
GO:0043604	amide biosynthetic process	7.48E-04	6.05E-02	1.37	Process
GO:0009889	regulation of biosynthetic process	7.92E-04	6.29E-02	1.15	Process
GO:0019219	regulation of nucleobase-containing compound metabolic process	7.98E-04	6.23E-02	1.16	Process
GO:0010941	regulation of cell death	9.00E-04	6.90E-02	1.34	Process
GO:0031326	regulation of cellular biosynthetic process	9.42E-04	7.10E-02	1.15	Process
GO:0005515	protein binding	2.31E-09	2.90E-06	1.20	Function

Table S14. Cont'd.

GO term	Description	*P*-value[1]	FDR *Q*-value	Enrichment	Category
GO:0003723	RNA binding	9.19E-05	5.77E-02	1.26	Function
GO:0005198	structural molecule activity	4.34E-04	1.82E-01	1.30	Function
GO:0005488	binding	6.48E-04	2.03E-01	1.06	Function
GO:0044424	intracellular part	1.81E-19	1.48E-16	1.14	Component
GO:0032991	protein-containing complex	4.49E-16	1.84E-13	1.25	Component
GO:0044464	cell part	4.17E-09	1.14E-06	1.08	Component
GO:0044446	intracellular organelle part	7.70E-09	1.58E-06	1.18	Component
GO:0043229	intracellular organelle	8.34E-09	1.37E-06	1.14	Component
GO:0043226	organelle	1.87E-08	2.56E-06	1.14	Component
GO:0044444	cytoplasmic part	2.74E-08	3.20E-06	1.16	Component
GO:0043227	membrane-bounded organelle	4.22E-08	4.32E-06	1.15	Component
GO:0044422	organelle part	9.98E-08	9.09E-06	1.16	Component
GO:0043231	intracellular membrane-bounded organelle	1.85E-06	1.52E-04	1.14	Component
GO:0044428	nuclear part	1.16E-05	8.63E-04	1.21	Component
GO:0044445	cytosolic part	1.79E-05	1.22E-03	1.60	Component
GO:1902494	catalytic complex	2.41E-05	1.52E-03	1.24	Component
GO:0005634	nucleus	1.71E-04	1.00E-02	1.15	Component
GO:0098796	membrane protein complex	3.25E-04	1.78E-02	1.29	Component
GO:0044451	nucleoplasm part	4.38E-04	2.24E-02	1.34	Component
GO:0098798	mitochondrial protein complex	7.48E-04	3.61E-02	1.37	Component

Table S14. Cont'd.

GO term	Description	*P*-value[1]	FDR *Q*-value	Enrichment	Category
GO:0005575	cellular_component	7.65E-04	3.48E-02	1.02	Component
GO:0098800	inner mitochondrial membrane protein complex	9.96E-04	4.30E-02	1.52	Component

[1] Only GO terms with *P*-value ≤ 0.001 are listed.

Table S15. Enriched GO terms in functional genes on the neo-Y in *Drosophila albomicans*.

GO term	Description	*P*-value[1]	FDR *Q*-value	Enrichment	Category
GO:0044237	cellular metabolic process	6.06E-11	3.41E-07	1.06	Process
GO:0008152	metabolic process	9.79E-10	2.75E-06	1.05	Process
GO:0071704	organic substance metabolic process	1.65E-08	3.09E-05	1.05	Process
GO:0044238	primary metabolic process	2.14E-08	3.02E-05	1.06	Process
GO:0006807	nitrogen compound metabolic process	5.74E-08	6.46E-05	1.06	Process
GO:0044260	cellular macromolecule metabolic process	5.96E-07	5.59E-04	1.08	Process
GO:0043170	macromolecule metabolic process	4.48E-06	3.60E-03	1.05	Process
GO:0043603	cellular amide metabolic process	9.48E-06	6.67E-03	1.16	Process
GO:0034641	cellular nitrogen compound metabolic process	1.01E-05	6.31E-03	1.07	Process
GO:1901564	organonitrogen compound metabolic process	1.02E-05	5.76E-03	1.06	Process
GO:0043604	amide biosynthetic process	5.47E-05	2.80E-02	1.18	Process
GO:0044281	small molecule metabolic process	6.96E-05	3.26E-02	1.10	Process
GO:0006518	peptide metabolic process	7.28E-05	3.15E-02	1.16	Process
GO:0009058	biosynthetic process	7.72E-05	3.10E-02	1.08	Process
GO:0009987	cellular process	1.04E-04	3.92E-02	1.02	Process
GO:0071702	organic substance transport	1.20E-04	4.22E-02	1.10	Process
GO:1901576	organic substance biosynthetic process	1.34E-04	4.44E-02	1.08	Process
GO:1901575	organic substance catabolic process	1.61E-04	5.03E-02	1.09	Process
GO:0008104	protein localization	2.07E-04	6.12E-02	1.10	Process
GO:0032787	monocarboxylic acid metabolic process	2.07E-04	5.82E-02	1.17	Process

Table S15. Cont'd.

GO term	Description	*P*-value[1]	FDR *Q*-value	Enrichment	Category
GO:0044267	cellular protein metabolic process	2.12E-04	5.69E-02	1.07	Process
GO:0071705	nitrogen compound transport	2.30E-04	5.88E-02	1.11	Process
GO:0042886	amide transport	2.35E-04	5.75E-02	1.13	Process
GO:0009056	catabolic process	2.56E-04	5.99E-02	1.09	Process
GO:0033036	macromolecule localization	2.74E-04	6.17E-02	1.10	Process
GO:0044249	cellular biosynthetic process	3.37E-04	7.30E-02	1.08	Process
GO:0006412	translation	3.39E-04	7.06E-02	1.17	Process
GO:0043043	peptide biosynthetic process	3.39E-04	6.81E-02	1.17	Process
GO:0015833	peptide transport	3.43E-04	6.66E-02	1.12	Process
GO:0045184	establishment of protein localization	3.55E-04	6.66E-02	1.12	Process
GO:0043436	oxoacid metabolic process	3.58E-04	6.50E-02	1.12	Process
GO:0006082	organic acid metabolic process	3.58E-04	6.30E-02	1.12	Process
GO:0015031	protein transport	3.89E-04	6.64E-02	1.12	Process
GO:0006631	fatty acid metabolic process	3.97E-04	6.57E-02	1.19	Process
GO:0019538	protein metabolic process	4.46E-04	7.17E-02	1.05	Process
GO:0006396	RNA processing	5.21E-04	8.15E-02	1.11	Process
GO:1901566	organonitrogen compound biosynthetic process	6.48E-04	9.86E-02	1.10	Process
GO:0044248	cellular catabolic process	6.62E-04	9.80E-02	1.08	Process
GO:0044282	small molecule catabolic process	7.67E-04	1.11E-01	1.17	Process
GO:0019752	carboxylic acid metabolic process	8.14E-04	1.15E-01	1.11	Process

Table S15. Cont'd.

GO term	Description	*P*-value[1]	FDR *Q*-value	Enrichment	Category
GO:0016054	organic acid catabolic process	9.72E-04	1.33E-01	1.19	Process
GO:0046395	carboxylic acid catabolic process	9.72E-04	1.30E-01	1.19	Process
GO:0003824	catalytic activity	4.84E-07	8.84E-04	1.05	Function
GO:0016887	ATPase activity	2.24E-05	2.04E-02	1.19	Function
GO:0016817	hydrolase activity, acting on acid anhydrides	4.32E-05	2.63E-02	1.13	Function
GO:0016818	hydrolase activity, acting on acid anhydrides, in phosphorus-containing anhydrides	4.32E-05	1.97E-02	1.13	Function
GO:0016462	pyrophosphatase activity	4.93E-05	1.80E-02	1.13	Function
GO:0017111	nucleoside-triphosphatase activity	1.24E-04	3.76E-02	1.13	Function
GO:0016740	transferase activity	4.16E-04	1.09E-01	1.07	Function
GO:0042623	ATPase activity, coupled	6.79E-04	1.55E-01	1.19	Function
GO:0043168	anion binding	7.39E-04	1.50E-01	1.07	Function
GO:0003723	RNA binding	9.08E-04	1.66E-01	1.09	Function
GO:0036094	small molecule binding	9.48E-04	1.57E-01	1.07	Function
GO:0044424	intracellular part	7.52E-14	7.68E-11	1.05	Component
GO:0044444	cytoplasmic part	1.89E-10	9.68E-08	1.07	Component
GO:0032991	protein-containing complex	9.28E-08	3.16E-05	1.07	Component
GO:0044422	organelle part	2.50E-07	6.38E-05	1.06	Component
GO:0044446	intracellular organelle part	2.74E-07	5.60E-05	1.06	Component
GO:0044464	cell part	1.00E-06	1.71E-04	1.03	Component
GO:0005737	cytoplasm	9.58E-06	1.40E-03	1.07	Component

Table S15. Cont'd.

GO term	Description	*P*-value[1]	FDR *Q*-value	Enrichment	Category
GO:1902494	catalytic complex	4.50E-05	5.75E-03	1.09	Component
GO:0098588	bounding membrane of organelle	4.69E-04	5.33E-02	1.16	Component
GO:0044429	mitochondrial part	8.05E-04	8.23E-02	1.10	Component

[1] Only GO terms with *P*-value ≤ 0.001 are listed.

Table S16. Enriched GO terms in functional genes on the neo-Y in *Drosophila americana*.

GO term	Description	*P*-value[1]	FDR *Q*-value	Enrichment	Category
GO:0044237	cellular metabolic process	2.30E-08	1.05E-04	1.08	Process
GO:0006807	nitrogen compound metabolic process	8.66E-07	1.97E-03	1.08	Process
GO:0008152	metabolic process	1.42E-05	2.15E-02	1.06	Process
GO:0043170	macromolecule metabolic process	2.67E-05	3.03E-02	1.07	Process
GO:0044249	cellular biosynthetic process	2.83E-05	2.57E-02	1.13	Process
GO:0034641	cellular nitrogen compound metabolic process	3.99E-05	3.02E-02	1.10	Process
GO:0044260	cellular macromolecule metabolic process	5.68E-05	3.69E-02	1.09	Process
GO:0009058	biosynthetic process	1.23E-04	6.99E-02	1.11	Process
GO:1901360	organic cyclic compound metabolic process	1.34E-04	6.77E-02	1.10	Process
GO:1901576	organic substance biosynthetic process	1.58E-04	7.19E-02	1.11	Process
GO:0006725	cellular aromatic compound metabolic process	1.89E-04	7.80E-02	1.10	Process
GO:0044238	primary metabolic process	2.00E-04	7.59E-02	1.06	Process
GO:0009059	macromolecule biosynthetic process	2.09E-04	7.31E-02	1.16	Process
GO:1901564	organonitrogen compound metabolic process	2.11E-04	6.85E-02	1.08	Process
GO:0006139	nucleobase-containing compound metabolic process	2.77E-04	8.40E-02	1.10	Process
GO:0046483	heterocycle metabolic process	2.87E-04	8.16E-02	1.10	Process
GO:0044271	cellular nitrogen compound biosynthetic process	2.96E-04	7.91E-02	1.15	Process
GO:1901566	organonitrogen compound biosynthetic process	3.56E-04	8.99E-02	1.16	Process
GO:0016070	RNA metabolic process	4.05E-04	9.68E-02	1.13	Process
GO:0071704	organic substance metabolic process	4.36E-04	9.91E-02	1.05	Process

Table S16. Cont'd.

GO term	Description	*P*-value[1]	FDR *Q*-value	Enrichment	Category
GO:0034645	cellular macromolecule biosynthetic process	9.28E-04	2.01E-01	1.16	Process
GO:0003723	RNA binding	1.79E-04	2.33E-01	1.16	Function
GO:0044424	intracellular part	9.72E-10	8.04E-07	1.06	Component
GO:0044444	cytoplasmic part	1.34E-08	5.55E-06	1.10	Component
GO:0044422	organelle part	4.25E-06	1.17E-03	1.08	Component
GO:0032991	protein-containing complex	6.87E-06	1.42E-03	1.08	Component
GO:0044446	intracellular organelle part	1.02E-05	1.69E-03	1.08	Component
GO:0005737	cytoplasm	2.66E-05	3.67E-03	1.10	Component
GO:1990904	ribonucleoprotein complex	2.96E-04	3.50E-02	1.15	Component
GO:0044429	mitochondrial part	5.77E-04	5.96E-02	1.16	Component

[1] Only GO terms with *P*-value ≤ 0.001 are listed.

Table S17. Enriched GO terms in pseudogenes on the neo-Y in *Drosophila miranda*.

GO term	Description	*P*-value[1]	FDR *Q*-value	Enrichment	Category
GO:0051606	detection of stimulus	5.21E-06	2.32E-02	1.86	Process
GO:0009593	detection of chemical stimulus	1.86E-05	4.14E-02	1.99	Process
GO:0006811	ion transport	4.05E-04	6.00E-01	1.41	Process
GO:0030001	metal ion transport	5.86E-04	6.51E-01	1.65	Process
GO:0005216	ion channel activity	9.91E-08	1.24E-04	1.91	Function
GO:0038023	signaling receptor activity	2.21E-07	1.39E-04	1.77	Function
GO:0004888	transmembrane signaling receptor activity	5.62E-07	2.35E-04	1.80	Function
GO:0060089	molecular transducer activity	8.48E-07	2.66E-04	1.71	Function
GO:0022838	substrate-specific channel activity	1.20E-06	3.00E-04	1.82	Function
GO:0022803	passive transmembrane transporter activity	5.21E-06	1.09E-03	1.74	Function
GO:0015267	channel activity	5.21E-06	9.34E-04	1.74	Function
GO:0022839	ion gated channel activity	9.89E-06	1.55E-03	1.85	Function
GO:0022836	gated channel activity	9.89E-06	1.38E-03	1.85	Function
GO:0015075	ion transmembrane transporter activity	4.17E-05	5.24E-03	1.48	Function
GO:0004930	G protein-coupled receptor activity	7.29E-05	8.31E-03	2.20	Function
GO:0004252	serine-type endopeptidase activity	7.38E-05	7.72E-03	1.85	Function
GO:0008236	serine-type peptidase activity	7.38E-05	7.13E-03	1.85	Function
GO:0017171	serine hydrolase activity	7.38E-05	6.62E-03	1.85	Function
GO:0022834	ligand-gated channel activity	7.60E-05	6.36E-03	1.97	Function
GO:0015276	ligand-gated ion channel activity	7.60E-05	5.96E-03	1.97	Function

Table S17. Cont'd.

GO term	Description	*P*-value[1]	FDR *Q*-value	Enrichment	Category
GO:0022857	transmembrane transporter activity	8.33E-05	6.15E-03	1.39	Function
GO:0005215	transporter activity	9.73E-05	6.78E-03	1.37	Function
GO:0015318	inorganic molecular entity transmembrane transporter activity	3.78E-04	2.50E-02	1.41	Function
GO:0020037	heme binding	4.01E-04	2.52E-02	1.76	Function
GO:0046906	tetrapyrrole binding	4.01E-04	2.40E-02	1.76	Function
GO:0005261	cation channel activity	4.84E-04	2.76E-02	1.80	Function
GO:0016021	integral component of membrane	7.54E-06	6.18E-03	1.32	Component
GO:0005887	integral component of plasma membrane	9.36E-06	3.84E-03	1.60	Component
GO:0031226	intrinsic component of plasma membrane	9.36E-06	2.56E-03	1.60	Component
GO:0031224	intrinsic component of membrane	1.07E-05	2.19E-03	1.32	Component

[1] Only GO terms with *P*-value ≤ 0.001 are listed.

Table S18. Enriched GO terms in pseudogenes on the neo-Y in *Drosophila albomicans*.

GO term	Description	*P*-value[1]	FDR *Q*-value	Enrichment	Category
GO:0009593	detection of chemical stimulus	5.77E-17	3.25E-13	5.06	Process
GO:0051606	detection of stimulus	2.22E-14	6.24E-11	3.80	Process
GO:0050907	detection of chemical stimulus involved in sensory perception	9.88E-11	1.85E-07	5.13	Process
GO:0050906	detection of stimulus involved in sensory perception	1.28E-10	1.80E-07	4.33	Process
GO:0050911	detection of chemical stimulus involved in sensory perception of smell	7.11E-08	8.00E-05	5.01	Process
GO:0007186	G protein-coupled receptor signaling pathway	3.78E-06	3.54E-03	2.32	Process
GO:0007606	sensory perception of chemical stimulus	6.17E-05	4.96E-02	2.38	Process
GO:0006355	regulation of transcription, DNA-templated	2.11E-04	1.49E-01	1.39	Process
GO:2001141	regulation of RNA biosynthetic process	2.11E-04	1.32E-01	1.39	Process
GO:1903506	regulation of nucleic acid-templated transcription	2.11E-04	1.19E-01	1.39	Process
GO:0007600	sensory perception	4.61E-04	2.36E-01	1.93	Process
GO:0030154	cell differentiation	5.94E-04	2.79E-01	1.80	Process
GO:0051252	regulation of RNA metabolic process	8.68E-04	3.76E-01	1.33	Process
GO:0004888	transmembrane signaling receptor activity	4.68E-12	8.54E-09	2.84	Function
GO:0038023	signaling receptor activity	1.45E-11	1.33E-08	2.60	Function
GO:0060089	molecular transducer activity	2.83E-10	1.72E-07	2.43	Function
GO:0004930	G protein-coupled receptor activity	5.64E-09	2.57E-06	3.44	Function
GO:0004984	olfactory receptor activity	7.11E-08	2.60E-05	5.01	Function
GO:0022839	ion gated channel activity	1.59E-07	4.84E-05	3.10	Function
GO:0022836	gated channel activity	1.59E-07	4.15E-05	3.10	Function

Table S18. Cont'd.

GO term	Description	*P*-value[1]	FDR *Q*-value	Enrichment	Category
GO:0003700	DNA-binding transcription factor activity	7.22E-07	1.65E-04	1.91	Function
GO:0022834	ligand-gated channel activity	8.38E-07	1.70E-04	3.57	Function
GO:0015276	ligand-gated ion channel activity	8.38E-07	1.53E-04	3.57	Function
GO:0005216	ion channel activity	1.30E-06	2.16E-04	2.63	Function
GO:0000981	DNA-binding transcription factor activity, RNA polymerase II-specific	2.68E-06	4.07E-04	1.94	Function
GO:0022838	substrate-specific channel activity	3.15E-06	4.42E-04	2.52	Function
GO:0001653	peptide receptor activity	3.20E-06	4.17E-04	3.86	Function
GO:0000977	RNA polymerase II regulatory region sequence-specific DNA binding	3.33E-06	4.06E-04	1.94	Function
GO:0001012	RNA polymerase II regulatory region DNA binding	3.33E-06	3.81E-04	1.94	Function
GO:0004252	serine-type endopeptidase activity	4.15E-06	4.46E-04	2.44	Function
GO:0022803	passive transmembrane transporter activity	4.15E-06	4.21E-04	2.44	Function
GO:0015267	channel activity	4.15E-06	3.99E-04	2.44	Function
GO:0140110	transcription regulator activity	4.26E-06	3.89E-04	1.71	Function
GO:0008528	G protein-coupled peptide receptor activity	4.71E-06	4.10E-04	4.01	Function
GO:0000976	transcription regulatory region sequence-specific DNA binding	7.09E-06	5.89E-04	1.85	Function
GO:0044212	transcription regulatory region DNA binding	7.09E-06	5.63E-04	1.85	Function
GO:0001067	regulatory region nucleic acid binding	8.86E-06	6.74E-04	1.84	Function
GO:1990837	sequence-specific double-stranded DNA binding	1.08E-05	7.90E-04	1.80	Function
GO:0008188	neuropeptide receptor activity	1.93E-05	1.35E-03	3.91	Function
GO:0008236	serine-type peptidase activity	3.61E-05	2.44E-03	2.21	Function

Table S18. Cont'd.

GO term	Description	*P*-value[1]	FDR *Q*-value	Enrichment	Category
GO:0017171	serine hydrolase activity	3.61E-05	2.35E-03	2.21	Function
GO:0008527	taste receptor activity	3.66E-05	2.31E-03	5.47	Function
GO:0003690	double-stranded DNA binding	4.36E-05	2.65E-03	1.72	Function
GO:0043565	sequence-specific DNA binding	4.51E-05	2.66E-03	1.67	Function
GO:0005261	cation channel activity	1.19E-04	6.81E-03	2.65	Function
GO:0003677	DNA binding	1.48E-04	8.21E-03	1.48	Function
GO:0005549	odorant binding	2.26E-04	1.21E-02	2.73	Function
GO:0000987	proximal promoter sequence-specific DNA binding	2.45E-04	1.28E-02	1.80	Function
GO:0000978	RNA polymerase II proximal promoter sequence-specific DNA binding	4.63E-04	2.35E-02	1.77	Function
GO:0032590	dendrite membrane	3.62E-07	3.70E-04	4.97	Component
GO:0032589	neuron projection membrane	3.20E-06	1.63E-03	3.86	Component
GO:0031256	leading edge membrane	3.20E-06	1.09E-03	3.86	Component
GO:0031253	cell projection membrane	1.09E-05	2.79E-03	3.39	Component
GO:0044459	plasma membrane part	4.56E-04	9.32E-02	1.46	Component

[1] Only GO terms with *P*-value ≤ 0.001 are listed.

Table S19. Enriched GO terms in pseudogenes on the neo-Y in *Drosophila americana*.

GO term	Description	*P*-value[1]	FDR *Q*-value	Enrichment	Category
GO:0045935	positive regulation of nucleobase-containing compound metabolic process	2.23E-04	1.00E+00	1.92	Process
GO:0050907	detection of chemical stimulus involved in sensory perception	2.34E-04	5.32E-01	4.04	Process
GO:0009593	detection of chemical stimulus	2.34E-04	3.55E-01	4.04	Process
GO:0007606	sensory perception of chemical stimulus	3.66E-04	4.16E-01	2.85	Process
GO:0009891	positive regulation of biosynthetic process	3.92E-04	3.56E-01	1.84	Process
GO:0031328	positive regulation of cellular biosynthetic process	3.92E-04	2.97E-01	1.84	Process
GO:0045944	positive regulation of transcription by RNA polymerase II	3.94E-04	2.56E-01	2.14	Process
GO:0007617	mating behavior	6.52E-04	3.71E-01	3.63	Process
GO:0051254	positive regulation of RNA metabolic process	7.12E-04	3.59E-01	1.85	Process
GO:0010557	positive regulation of macromolecule biosynthetic process	9.39E-04	4.27E-01	1.80	Process
GO:0050911	detection of chemical stimulus involved in sensory perception of smell	9.67E-04	4.00E-01	3.89	Process
GO:0016298	lipase activity	1.32E-05	1.72E-02	3.46	Function
GO:0043565	sequence-specific DNA binding	7.17E-05	4.69E-02	1.86	Function
GO:0000976	transcription regulatory region sequence-specific DNA binding	1.60E-04	6.97E-02	1.88	Function
GO:0001067	regulatory region nucleic acid binding	2.05E-04	6.71E-02	1.85	Function
GO:0044212	transcription regulatory region DNA binding	2.05E-04	5.37E-02	1.85	Function
GO:0015280	ligand-gated sodium channel activity	2.59E-04	5.64E-02	5.19	Function
GO:0022834	ligand-gated channel activity	2.65E-04	4.95E-02	3.34	Function
GO:0015276	ligand-gated ion channel activity	2.65E-04	4.33E-02	3.34	Function

Table S19. Cont'd.

GO term	Description	*P*-value[1]	FDR *Q*-value	Enrichment	Category
GO:1990837	sequence-specific double-stranded DNA binding	3.32E-04	4.83E-02	1.81	Function
GO:0003690	double-stranded DNA binding	4.28E-04	5.60E-02	1.77	Function
GO:0060089	molecular transducer activity	4.61E-04	5.47E-02	2.08	Function
GO:0000977	RNA polymerase II regulatory region sequence-specific DNA binding	6.08E-04	6.62E-02	1.82	Function
GO:0001012	RNA polymerase II regulatory region DNA binding	6.08E-04	6.11E-02	1.82	Function
GO:0003700	DNA-binding transcription factor activity	6.28E-04	5.86E-02	1.79	Function
GO:0052689	carboxylic ester hydrolase activity	6.39E-04	5.56E-02	2.72	Function
GO:0038023	signaling receptor activity	6.47E-04	5.28E-02	2.12	Function
GO:0004984	olfactory receptor activity	9.67E-04	7.44E-02	3.89	Function
GO:0030312	external encapsulating structure	5.51E-05	4.56E-02	4.15	Component
GO:0005887	integral component of plasma membrane	7.18E-05	2.97E-02	2.03	Component
GO:0031226	intrinsic component of plasma membrane	1.29E-04	3.55E-02	1.97	Component
GO:0016021	integral component of membrane	3.18E-04	6.58E-02	1.51	Component
GO:0031224	intrinsic component of membrane	4.97E-04	8.21E-02	1.48	Component
GO:0044421	extracellular region part	5.41E-04	7.45E-02	1.71	Component

[1] Only GO terms with *P*-value ≤ 0.001 are listed.

Table S20. Possible functions of the 35 genes that have parallelly been pseudogenized on the neo-Ys in *Drosophila miranda* and *D. albomicans* based on the *D. melanogaster* orthologs.

No.[1]	Flybase ID[2]	Symbol[2]	Gene snapshot[2]
1	FBgn0001187	*Hex-C*	A hexokinase involved in glucose homeostasis
2	FBgn0001319	*kn*	A transcription factor required for somatic and alary muscle specification and embryonic head segmentation
3	FBgn0011659	*Mlh1*	-
4	FBgn0013763	*Idgf6*	A secreted protein that is highly expressed in larval fat body and adult head, and also involved in molting and egg chamber tube morphogenesis
5	FBgn0020269	*mspo*	-
6	FBgn0025827	*CG6421*	-
7	FBgn0028424	*JhI-26*	A sperm protein, overexpression of which causes upregulation of the male accessory gland protein gene, higher embryonic lethality, and reduction of receptivity to remating in mated females
8	FBgn0028743	*Dhit*	A protein that negatively regulates Galpha signaling and is involved in several GPCR-mediated signaling and developmental programs, such as asymmetric cell division in the sensory organ lineage
9	FBgn0033128	*Tsp42Eg*	-
10	FBgn0033540	*Elp2*	-
11	FBgn0033661	*CG13185*	-
12	FBgn0033708	*CG8850*	-
13	FBgn0033744	*Dh44-R2*	A protein that exhibits diuretic hormone receptor activity and is involved in G protein-coupled receptor signaling pathways, hormone-mediated signaling pathways, and response to salt stress
14	FBgn0033948	*CG12863*	-
15	FBgn0034136	*DAT*	A dopamine transporter that mediates uptake of dopamine from the synaptic cleft, loss of which increases extracellular dopamine and is associated with behavioral phenotypes including increased activity and decreased sleep
16	FBgn0034166	*CG6472*	-
17	FBgn0034177	*AsnRS-m*	-

Table S20. Cont'd.

No.[1]	Flybase ID[2]	Symbol[2]	Gene snapshot[2]
18	FBgn0034232	*CG4866*	-
19	FBgn0034314	*nopo*	A RING domain-containing E3 ubiquitin ligase that is essential for early embryogenesis and positively regulates caspase-dependent cell death
20	FBgn0034452	*Oseg6*	-
21	FBgn0034567	*CG15651*	-
22	FBgn0034623	*CG9822*	-
23	FBgn0034624	*CG17974*	-
24	FBgn0034634	*CG10494*	-
25	FBgn0035025	*uri*	-
26	FBgn0042083	*Mccc2*	-
27	FBgn0046879	*Obp56c*	-
28	FBgn0050411	*CG30411*	-
29	FBgn0053544	*Vkor*	An enzyme that converts Vitamin-K 2,3-epoxide back to the active form of Vitamin-K by de-epoxidation
30	FBgn0082585	*sprt*	-
31	FBgn0262816	*CG43187*	-
32	FBgn0263020	*CG43315*	-

[1] For other three genes, orthologs were not detected in *D. melanogaster* based on the BLASTP search.

[2] Information are retrieved from FlyBase (https://flybase.org/).

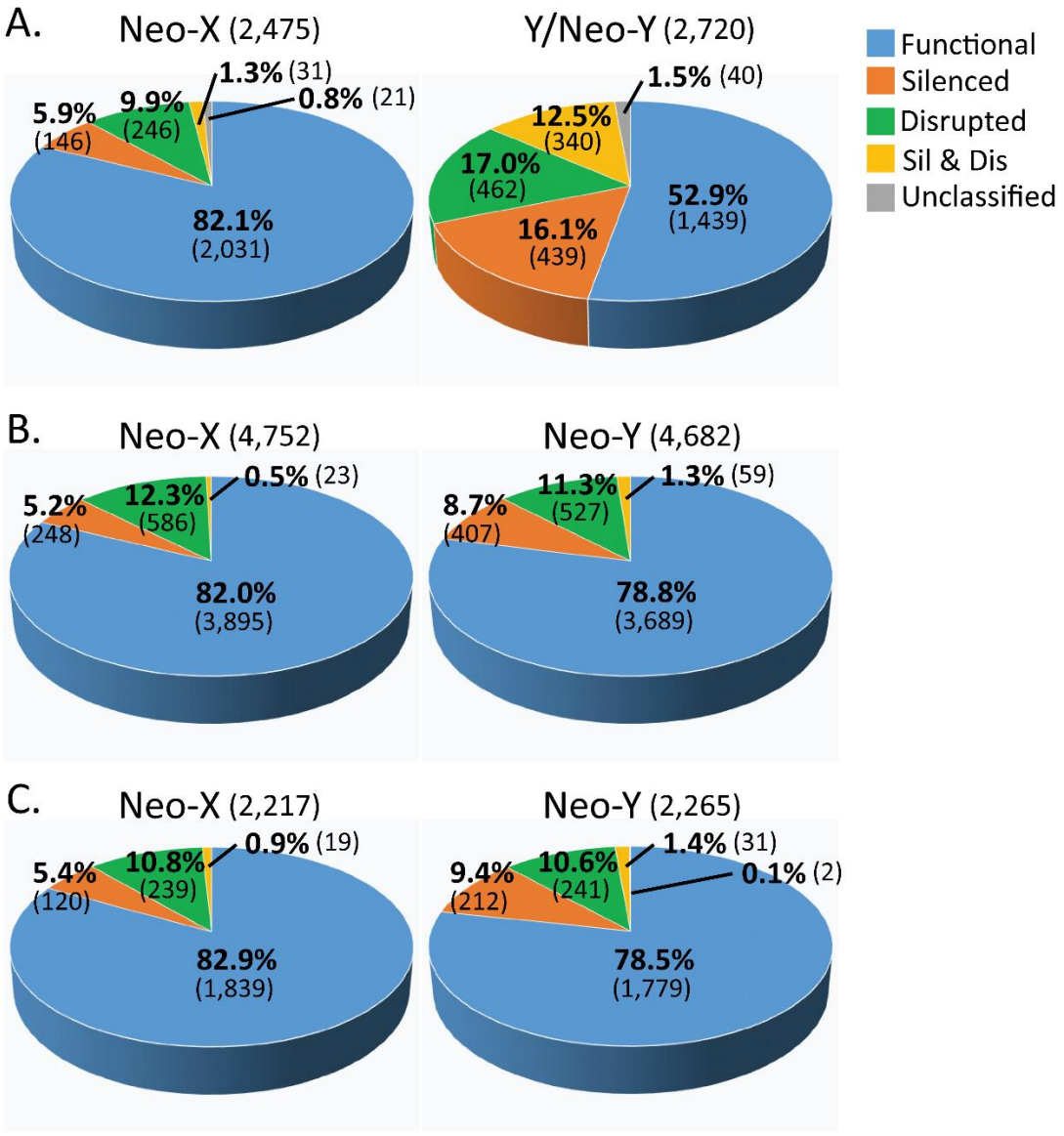

Fig. S1: Classification of neo-X and neo-Y gene groups in (A) *Drosophila miranda*, (B) *D. albomicans*, and (C) *D. americana*. For each category, all inparalogs were regarded as a single gene group (see *SUPPLEMENTARY METHODS* for the procedure to detect inparalogs). Numbers in parentheses indicate the numbers of gene groups in each category. Colors on each pie chart correspond to the categories shown on the top-right corner. Silenced, disrupted, and silenced-and-disrupted genes are pseudogenes.

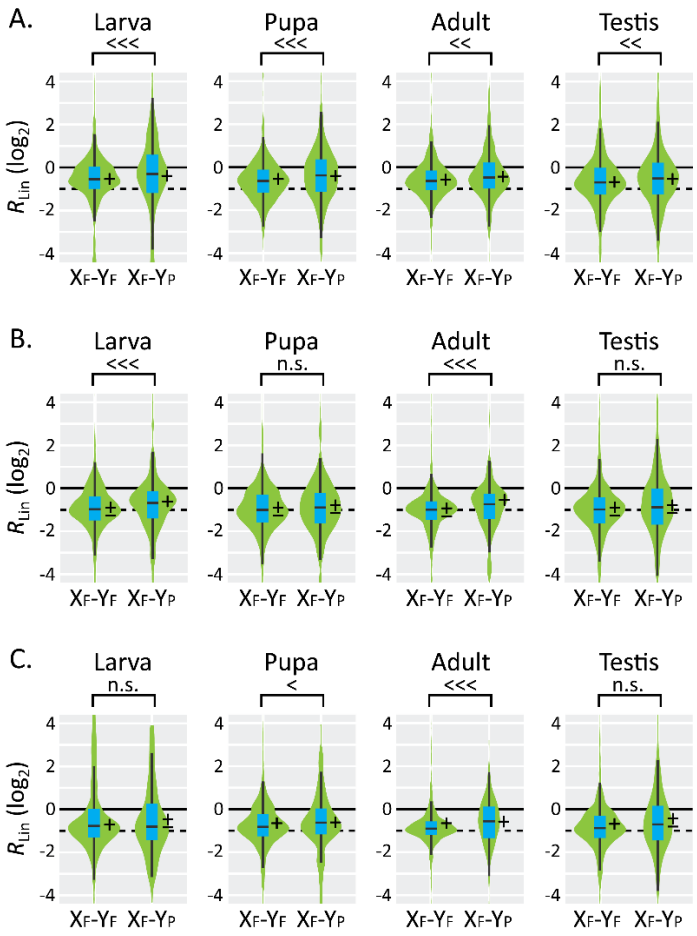

Fig. S2: Relationship between the functionality of neo-Y-linked genes and the DC of neo-X-linked homologs in larva, pupa, adult, and testis of (A) *Drosophila miranda*, (B) *D. albomicans*, and (C) *D. americana*. To compute R_{Lin}, the cTPM value (corrected TPM, TPM normalized by median) was used. X_F-Y_F, a group of genes with functional neo-X-linked and neo-Y-linked homologs; X_F-Y_P, a group of genes with functional neo-X-linked homologs and pseudogenized neo-Y-linked homologs. In the X_F-Y_F and X_F-Y_P groups, 664 and 435 genes, respectively, were analyzed for *D. miranda*, 2,449 and 218 for *D. albomicans*, and 1,204 and 93 for *D. americana*. A box plot is also shown on each violin plot. Differences of R_{Lin} values between groups were tested based on a permutation test with 10,000 replicates with the correction of multiple testing by the Benjamini and Hochberg method (Benjamini and Hochberg 1995) under the null hypothesis of R_{Lin} (X_F-Y_F) = R_{Lin} (X_F-Y_P): <<<, Q<0.001; <<, Q<0.01; <, Q<0.05; n.s., Q≥0.05. A solid line indicates the R_{Lin} value of 1 (0 in $\log_2$) indicating perfect DC, whereas a broken line corresponds to a value of 0.5 (−1 in $\log_2$) indicating no DC. +, –, and ± along each plot means that the median R_{Lin} value is >0.5, <0.5, and 0.5 at the 5% significance level, respectively, based on a bootstrap test with 10,000 replications with the correction of multiple testing.

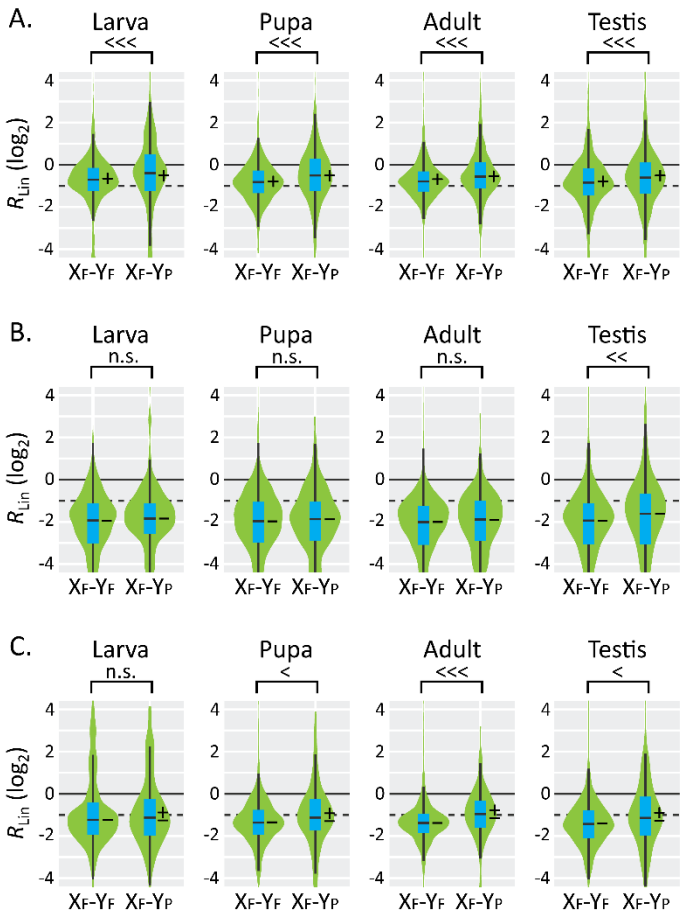

Fig. S3: Relationship between the functionality of neo-Y-linked genes and the DC of neo-X-linked homologs in the larva, pupa, adult, and testis of (A) *Drosophila miranda*, (B) *D. albomicans*, and (C) *D. americana*. For computing R_{Lin}, the corrected fragments per kilobase of exon per million mapped reads (cFPKM, FPKM normalized by median) was used. Only uniquely mapped reads were used for computing cFPKM. X_F-Y_F, a group of genes with functional neo-X-linked and neo-Y-linked homologs; X_F-Y_P, a group of genes with functional neo-X-linked homologs and pseudogenized neo-Y-linked homologs. In the X_F-Y_F and X_F-Y_P groups, 664 and 435 genes, respectively, were analyzed for *D. miranda*, 2,449 and 218 for *D. albomicans*, and 1,204 and 93 for *D. americana*. A box plot is also shown on each violin plot. Differences of R_{Lin} values between groups were tested based on a permutation test with 10,000 replicates with the correction of multiple testing by the Benjamini and Hochberg method (Benjamini and Hochberg 1995) under the null hypothesis of R_{Lin} (X_F-Y_F) = R_{Lin} (X_F-Y_P): <<<, Q<0.001; <<, Q<0.01; <, Q<0.05; n.s., Q≥0.05. A solid line indicates the R_{Lin} value of 1 (0 in $\log_2$) indicating perfect DC, whereas a broken line corresponds to a value of 0.5 (−1 in $\log_2$) indicating no DC. +, –, and ± along each plot means that the median R_{Lin} value is >0.5, <0.5, and 0.5 at the 5% significance level, respectively, based on a bootstrap test with 10,000 replications with the correction of multiple testing.

A.

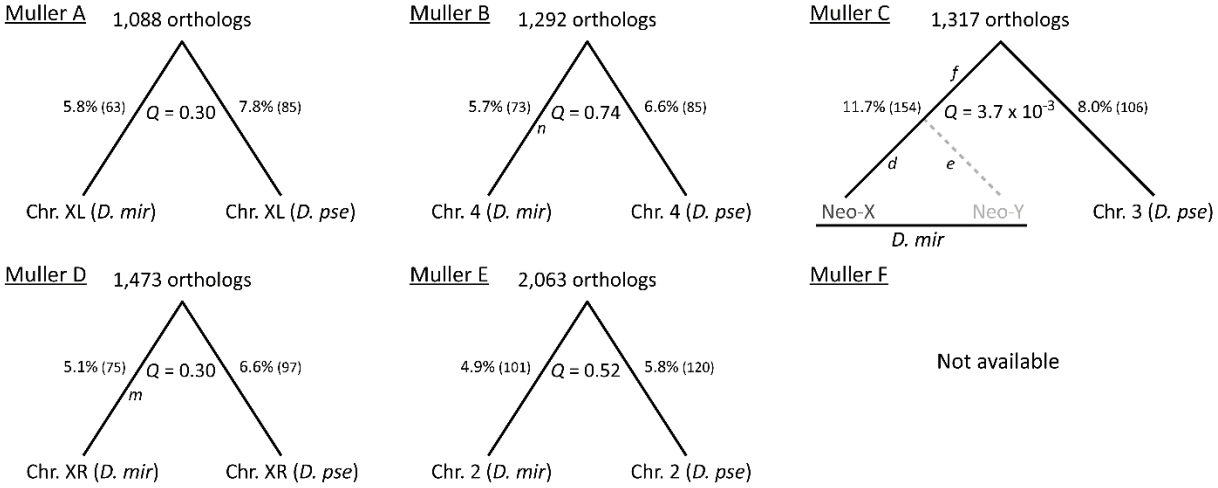
Muller A
1,088 orthologs
5.8% (63)
Q = 0.30
7.8% (85)
Chr. XL (D. mir)
Chr. XL (D. pse)
Muller B
1,292 orthologs
5.7% (73)
n
Q = 0.74
6.6% (85)
Chr. 4 (D. mir)
Chr. 4 (D. pse)
Muller C
1,317 orthologs
f
11.7% (154)
Q = 3.7 x 10-3
8.0% (106)
d
e
Neo-X
Neo-Y
Chr. 3 (D. pse)
D. mir
Muller D
1,473 orthologs
5.1% (75)
Q = 0.30
6.6% (97)
m
Chr. XR (D. mir)
Chr. XR (D. pse)
Muller E
2,063 orthologs
4.9% (101)
Q = 0.52
5.8% (120)
Chr. 2 (D. mir)
Chr. 2 (D. pse)
Muller F
Not available

B.

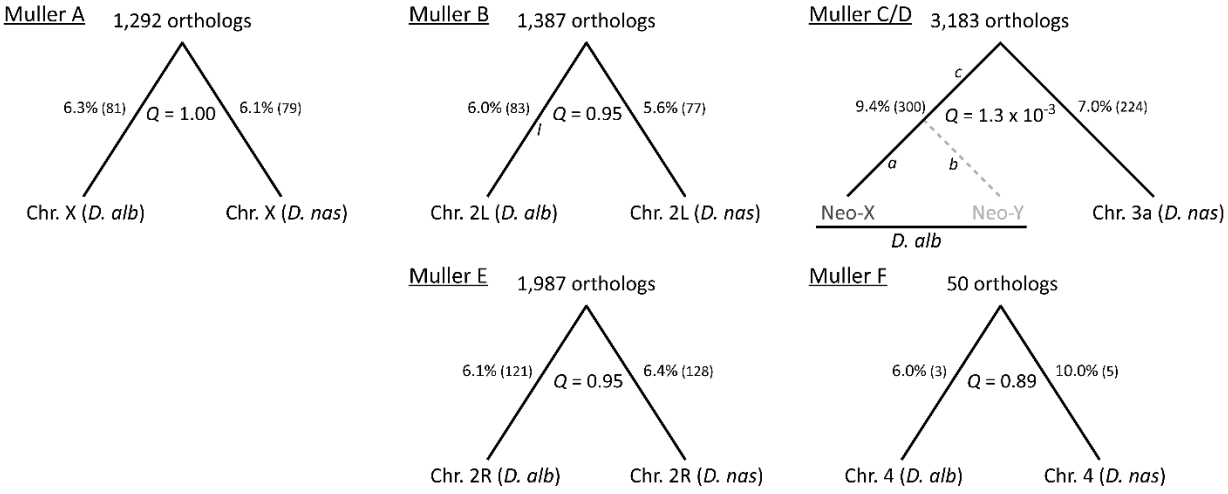
Muller A
1,292 orthologs
6.3% (81)
Q = 1.00
6.1% (79)
Chr. X (D. alb)
Chr. X (D. nas)
Muller B
1,387 orthologs
6.0% (83)
l
Q = 0.95
5.6% (77)
Chr. 2L (D. alb)
Chr. 2L (D. nas)
Muller C/D
3,183 orthologs
c
9.4% (300)
Q = 1.3 x 10-3
7.0% (224)
a
b
Neo-X
Neo-Y
Chr. 3a (D. nas)
D. alb
Muller E
1,987 orthologs
6.1% (121)
Q = 0.95
6.4% (128)
Chr. 2R (D. alb)
Chr. 2R (D. nas)
Muller F
50 orthologs
6.0% (3)
Q = 0.89
10.0% (5)
Chr. 4 (D. alb)
Chr. 4 (D. nas)

C.

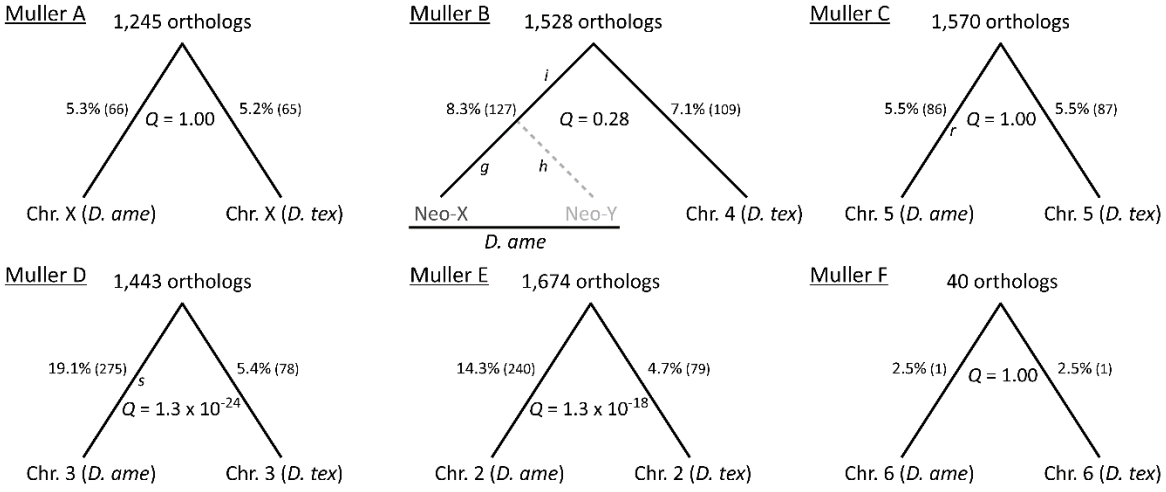
Muller A
1,245 orthologs
5.3% (66)
Q = 1.00
5.2% (65)
Chr. X (D. ame)
Chr. X (D. tex)
Muller B
1,528 orthologs
i
8.3% (127)
Q = 0.28
7.1% (109)
g
h
Neo-X
Neo-Y
Chr. 4 (D. tex)
D. ame
Muller C
1,570 orthologs
5.5% (86)
r
Q = 1.00
5.5% (87)
Chr. 5 (D. ame)
Chr. 5 (D. tex)
Muller D
1,443 orthologs
19.1% (275)
s
5.4% (78)
Q = 1.3 x 10-24
Chr. 3 (D. ame)
Chr. 3 (D. tex)
Muller E
1,674 orthologs
14.3% (240)
4.7% (79)
Q = 1.3 x 10-18
Chr. 2 (D. ame)
Chr. 2 (D. tex)
Muller F
40 orthologs
2.5% (1)
Q = 1.00
2.5% (1)
Chr. 6 (D. ame)
Chr. 6 (D. tex)

Fig. S4: Pseudogenization events in (A) *Drosophila miranda*, (B) *D. albomicans*, and (C) *D. americana* lineages compared with those in their closely related species, *D. pseudoobscura*, *D. nasuta*, and *D. texana*, respectively. Numbers in parentheses indicate the numbers of genes that were pseudogenized in each lineage. The orthologs that were regarded to be functional in the outgroup species (*D. obscura*, *D. kohkoa*, and *D. novamexicana*, respectively) and located on the same Muller element among the three species compared without any inparalogs were used for this analysis. The number of such orthologs is shown above each tree. Statistical significance in the difference of the pseudogenization rate between lineages leading to the species with neo-sex chromosomes and its closely related species was computed by χ^2 test with the correction of multiple testing under the null hypothesis of equal pseudogenization rates between lineages.

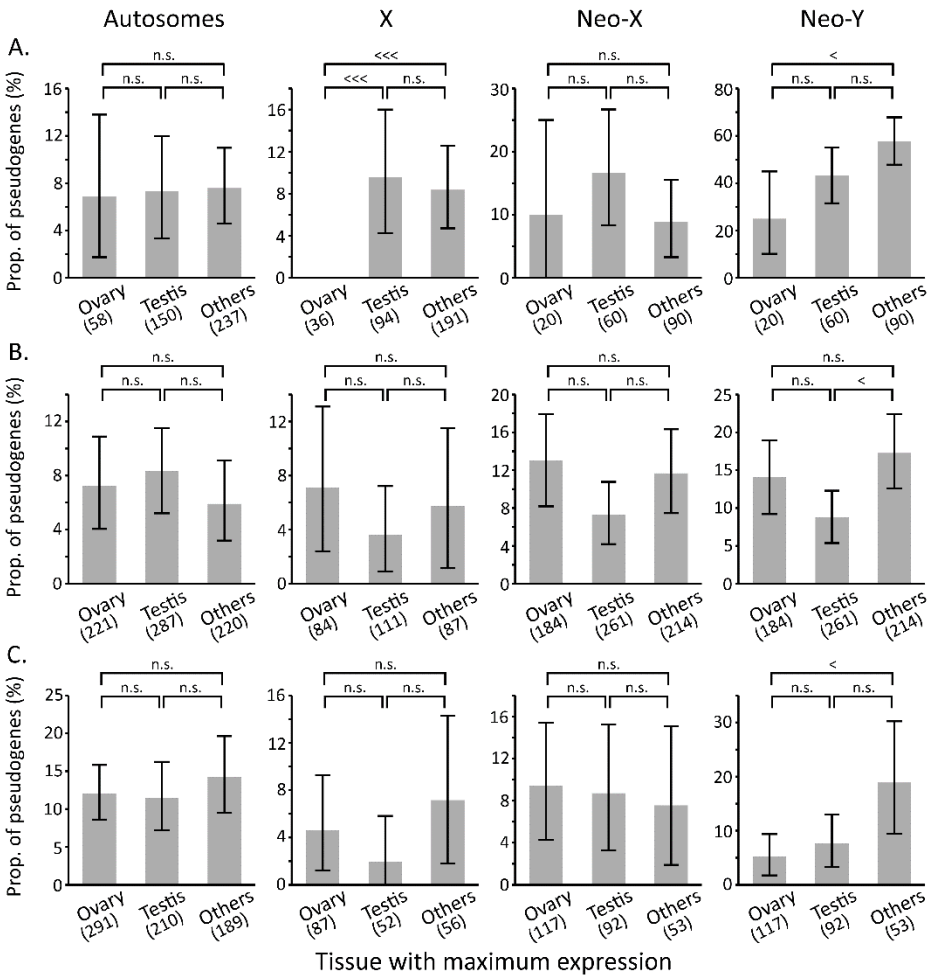

Fig. S5: Relationship between spatiotemporal gene expression pattern and pseudogenization. All genes were classified into three groups based on the tissue with the highest expression in (A) *Drosophila pseudoobscura*, (B) *D. nasuta*, and (C) *D. texana*, the closely related species of *D. miranda*, *D. albomicans*, and *D. americana*, respectively, based on the TPM value. However, to remove the genes with similar TPMs in multiple tissues, only genes with at least two-fold TPM in a tissue compared with that in the other tissues examined were used for this analysis. The orthologs regarded to be functional in the close relatives (*D. pseudoobscura* and *D. obscura* for *D. miranda*, *D. nasuta* and *D. kohkoa* for *D. albomicans*, and *D. texana* and *D. novamexicana* for *D. americana*, respectively) and located on the same Muller element without any inparalogs were used for this analysis. Number of genes in each category is shown in parenthesis. Error bars show the 95% confidence interval based on a bootstrap resampling with 10,000 replicates. Statistical significance between groups was tested by Fisher's exact test with correction for multiple testing: <<< or >>>, $Q<0.001$; << or >>; $Q<0.01$; < or >, $Q<0.05$; n.s., $Q\geq0.05$.

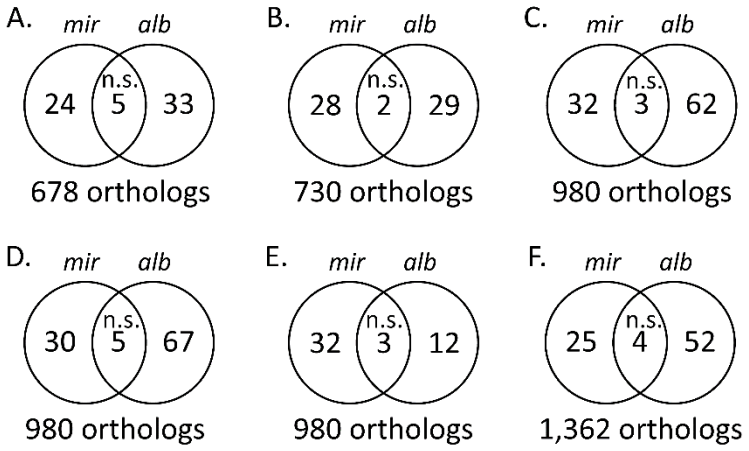

Fig. S6: Lineage-specific and parallel (shared) pseudogenization events on Muller elements (A) A, (B) B, (C-E) D, and (F) E in the lineages of *Drosophila miranda* (*mir*) and *D. albomicans* (*alb*). Muller element D is the Chromosome XR in *D. miranda* whereas it is also the neo-sex chromosomes in *D. albomicans*. Therefore, for Muller element D, branches (C) *m* and *a*, (D) *m* and *b*, and (E) *m* and *c* in Fig. S4 were separately analyzed. Each Venn diagram shows the number of pseudogenization events in the two lineages. The number of orthologs regarded to be functional in the outgroup species (*D. obscura* and *D. kohkoa*, respectively) and located on the same Muller element without any inparalogs is shown below each diagram. Statistical difference between the observed and expected numbers of parallel pseudogenizations was tested by a binomial test with correction for multiple testing: n.s., $Q \geq 0.05$.

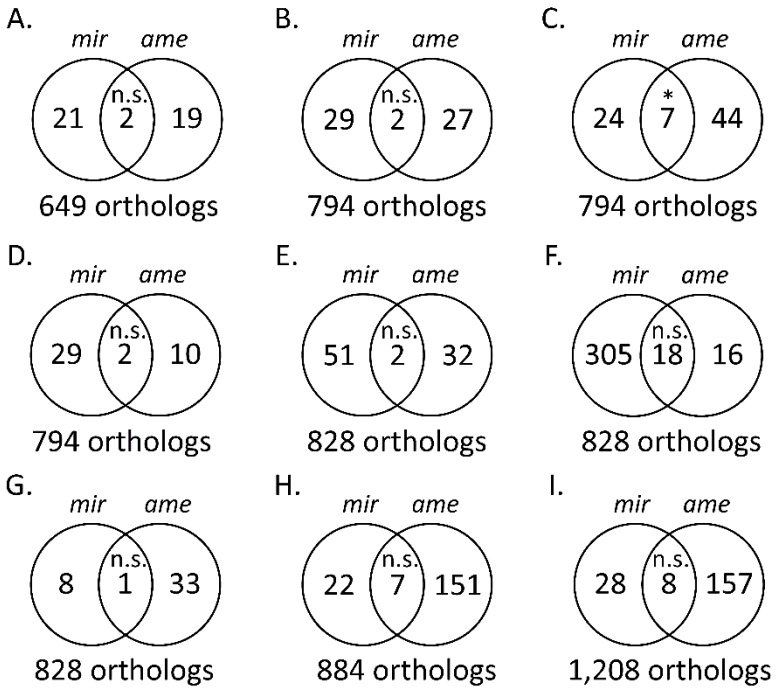

Fig. S7: Lineage-specific and parallel (shared) pseudogenization events on Muller elements (A) A, (B-D) B, (E-G) C, (H) D, and (I) E in the lineages of *Drosophila miranda* (*mir*) and *D. americana* (*ame*). Muller element B is the Chromosome 4 in *D. miranda* whereas it is the neo-sex chromosomes in *D. americana*. Therefore, for this Muller element, branches (B) *n* and *g*, (C) *n* and *h*, and (D) *n* and *i* in Fig. S4 were separately analyzed. Similarly, Muller element C is the neo-sex chromosomes in *D. miranda* whereas it is the Chromosome 5 in *D. americana*. Therefore, for this Muller element, branches (E) *d* and *r*, (F) *e* and *r*, and (G) *f* and *r* in Fig. S4 were separately analyzed. Each Venn diagram shows the number of pseudogenization events in the two lineages. The number of orthologs regarded to be functional in the outgroup species (*D. obscura* and *D. novamexicana*, respectively) and located on the same Muller element without any inparalogs is shown below each diagram. Statistical difference between the observed and expected numbers of parallel pseudogenizations was tested by a binomial test with correction for multiple testing: *, $Q < 0.05$; n.s., $Q \geq 0.05$.

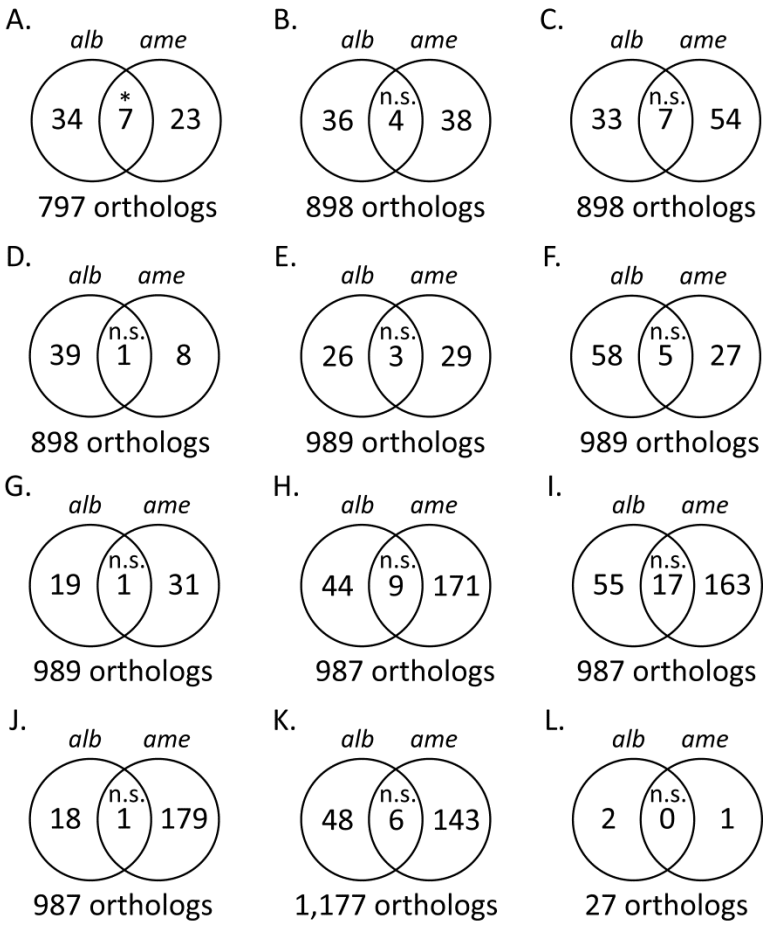

Fig. S8: Lineage-specific and parallel (shared) pseudogenization events on Muller elements (A) A, (B-D) B, (E-G) C, (H-J) D, (K) E, and (L) F in the lineages of *Drosophila albomicans* (*alb*) and *D. americana* (*ame*). Muller element B is the Chromosome 2L in *D. albomicans* whereas it is the neo-sex chromosomes in *D. americana*. Therefore, for this Muller element, branches (B) *l* and *g*, (C) *l* and *h*, and (D) *l* and *i* in Fig. S4 were separately analyzed. Similarly, Muller elements C and D are the neo-sex chromosomes in *D. albomicans* whereas they are the Chromosomes 5 and 3, respectively, in *D. americana*. Therefore, for these Muller elements, branches (E) *a* and *r*, (F) *b* and *r*, (G) *c* and *r*, (H) *a* and *s*, (I) *b* and *s*, and (J) *c* and *s* in Fig. S4 were separately analyzed. Each Venn diagram shows the number of pseudogenization events in the two lineages. The number of orthologs regarded to be functional in the outgroup species (*D. kohkoa* and *D. novamexicana*, respectively) and located on the same Muller element without any inparalogs is shown below each diagram. Statistical difference between the observed and expected numbers of parallel pseudogenizations was tested by a binomial test with correction for multiple testing: *, $Q < 0.05$; n.s., $Q \geq 0.05$.

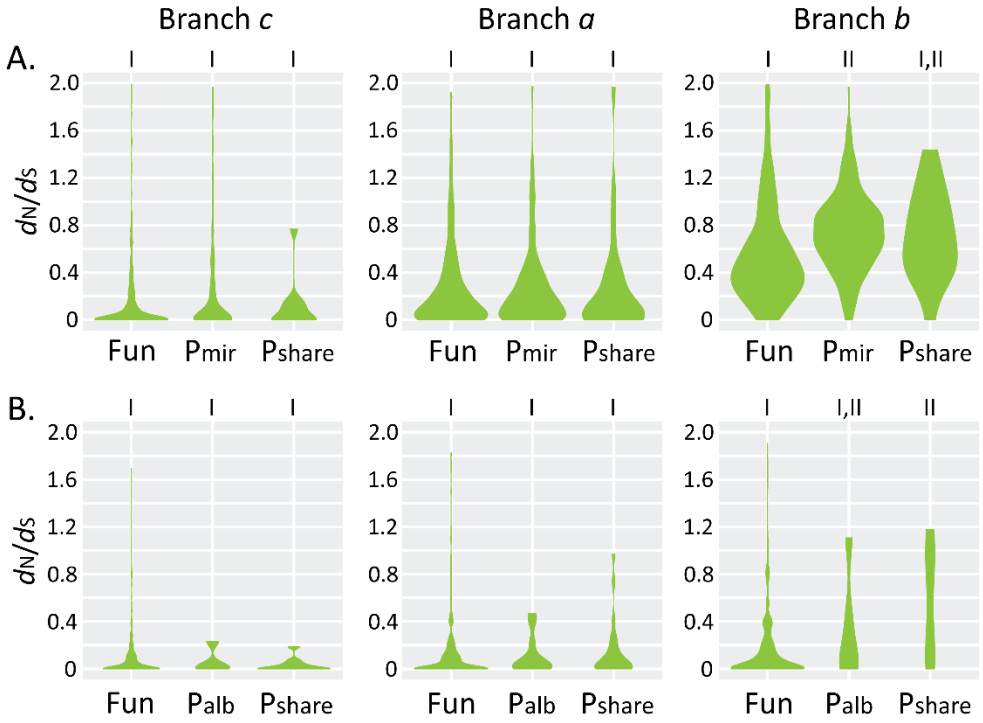

Fig. S9: Relationship between functionality of neo-Y-linked genes and ratio of nonsynonymous to synonymous nucleotide divergence per site (d_N/d_S) in (A) *Drosophila miranda* and (B) *D. albomicans* lineages. Branches *c* (left), *a* (center), and *b* (right) corresponds to those in Fig. 4. The orthologs regarded to be functional in the outgroup species (*D. obscura* and *D. kohkoa*, respectively) and located on Muller element C without any inparalogs were used. Fun, neo-Y-linked genes that are functional at least in (A) *D. miranda* or (B) *D. albomicans*; P_{mir}, neo-Y-linked genes that are nonfunctional in *D. miranda* but functional in *D. albomicans*; P_{alb}, neo-Y-linked genes that are nonfunctional in *D. albomicans* but functional in *D. miranda*; P_{share}, neo-Y-linked genes that are nonfunctional in both *D. miranda* and *D. albomicans*. Differences of d_N/d_S ratios between groups were evaluated by Mann-Whitney *U* test with correction for multiple testing under the null hypothesis of the equal d_N/d_S ratio. Same roman numerals indicate $Q \geq 0.05$, whereas different numerals mean $Q < 0.05$ between categories.

REFERENCES

Altschul SF, Madden TL, Schaffer AA, Zhang J, Zhang Z, Miller W, Lipman DJ. 1997. Gapped BLAST and PSI-BLAST: a new generation of protein database search programs. *Nucleic Acids Res* **25**: 3389-3402.

Benjamini H, Hochberg Y. 1995. Controlling the false discovery rate: a practical and powerful approach to multiple testing. *J R Statist Soc B* **57**: 289-300.

Chin CS, Alexander DH, Marks P, Klammer AA, Drake J, Heiner C, Clum A, Copeland A, Huddleston J, Eichler EE et al. 2013. Nonhybrid, finished microbial genome assemblies from long-read SMRT sequencing data. *Nat Methods* **10**: 563-569.

Cox MP, Peterson DA, Biggs PJ. 2010. SolexaQA: At-a-glance quality assessment of Illumina second-generation sequencing data. *BMC Bioinformatics* **11**: 485.

DePristo MA, Banks E, Poplin R, Garimella KV, Maguire JR, Hartl C, Philippakis AA, del Angel G, Rivas MA, Hanna M et al. 2011. A framework for variation discovery and genotyping using next-generation DNA sequencing data. *Nature Genetics* **43**: 491-498.

Dobin A, Davis CA, Schlesinger F, Drenkow J, Zaleski C, Jha S, Batut P, Chaisson M, Gingeras TR. 2013. STAR: ultrafast universal RNA-seq aligner. *Bioinformatics* **29**: 15-21.

Eden E, Navon R, Steinfeld I, Lipson D, Yakhini Z. 2009. GOrilla: a tool for discovery and visualization of enriched GO terms in ranked gene lists. *BMC Bioinformatics* **10**: 48.

Edgar RC. 2004. MUSCLE: multiple sequence alignment with high accuracy and high throughput. *Nucleic Acids Res* **32**: 1792-1797.

Haas BJ, Papanicolaou A, Yassour M, Grabherr M, Blood PD, Bowden J, Couger MB, Eccles D, Li B, Lieber M et al. 2013. De novo transcript sequence reconstruction from RNA-seq using the Trinity platform for reference generation and analysis. *Nat Protoc* **8**: 1494-1512.

Hatsumi M, Morishige Y, Wakahama K-I. 1988. Metaphase chromosomes of four species of the *Drosophila nasuta* subgroup. *Jpn J Genet* **63**: 435-444.

Kim D, Paggi JM, Park C, Bennett C, Salzberg SL. 2019. Graph-based genome alignment and genotyping with HISAT2 and HISAT-genotype. *Nat Biotechnol* **37**: 907-915.

Kitagawa O, Wakahama K-I, Fuyama Y, Shimada Y, Takanashi E, Hatsumi M, Uwabo M, Mita Y. 1982. Genetic studies of the *Drosophila nasuta* subgroup, with notes on distribution and morphology. *Jpn J Genet* **57**: 113-141.

Li B, Dewey CN. 2011. RSEM: accurate transcript quantification from RNA-Seq data with or without a reference genome. *BMC Bioinformatics* **12**: 323.

Li H, Durbin R. 2009. Fast and accurate short read alignment with Burrows-Wheeler transform. *Bioinformatics* **25**: 1754-1760.

Lin F, Xing K, Zhang J, He X. 2012. Expression reduction in mammalian X chromosome evolution refutes Ohno's hypothesis of dosage compensation. *Proc Natl Acad Sci USA* **109**: 11752-11757.

Mahajan S, Wei KH, Nalley MJ, Gibilisco L, Bachtrog D. 2018. De novo assembly of a young *Drosophila* Y chromosome using single-molecule sequencing and chromatin conformation capture. *PLoS Biol* **16**: e2006348.

Martin M. 2011. Cutadapt removes adapter sequences from high-throughput sequencing reads. *EMBnetjournal* **17**: 10-12.

Mortazavi A, Williams BA, McCue K, Schaeffer L, Wold B. 2008. Mapping and quantifying mammalian transcriptomes by RNA-Seq. *Nat Methods* **5**: 621-628.

Nozawa M, Ikeo K, Gojobori T. 2018. Gene-by-gene or localized dosage compensation on the neo-X chromosome in *Drosophila miranda*. *Genome Biol Evol* **10**: 1875-1881.

Nozawa M, Onizuka K, Fujimi M, Ikeo K, Gojobori T. 2016. Accelerated pseudogenization on the neo-X chromosome in *Drosophila miranda*. *Nat Commun* **7**: 13659.

Pertea M, Pertea GM, Antonescu CM, Chang TC, Mendell JT, Salzberg SL. 2015. StringTie enables improved reconstruction of a transcriptome from RNA-seq reads. *Nat Biotechnol* **33**: 290-295.

Ranwez V, Douzery EJP, Cambon C, Chantret N, Delsuc F. 2018. MACSE v2: Toolkit for the Alignment of Coding Sequences Accounting for Frameshifts and Stop Codons. *Mol Biol Evol* **35**: 2582-2584.

Richards S, Liu Y, Bettencourt BR, Hradecky P, Letovsky S, Nielsen R, Thornton K, Hubisz MJ, Chen R, Meisel RP et al. 2005. Comparative genome sequencing of *Drosophila pseudoobscura*: chromosomal, gene, and cis-element evolution. *Genome Res* **15**: 1-18.

Rzhetsky A, Nei M. 1993. Theoretical foundation of the minimum-evolution method of phylogenetic inference. *Mol Biol Evol* **10**: 1073-1095.

Sambrook J, Russell DW. 2001. *Molecular cloning: a laboratory manual*. Cold Spring Harbor Laboratory Press, New York.

Seppey M, Manni M, Zdobnov EM. 2019. BUSCO: assessing genome assembly and annotation completeness. *Methods Mol Biol* **1962**: 227-245.

Simao FA, Waterhouse RM, Ioannidis P, Kriventseva EV, Zdobnov EM. 2015. BUSCO: assessing genome assembly and annotation completeness with single-copy orthologs. *Bioinformatics* **31**: 3210-3212.

Stanke M, Waack S. 2003. Gene prediction with a hidden Markov model and a new intron submodel. *Bioinformatics* **19 Suppl 2**: ii215-225.

Wagner GP, Kin K, Lynch VJ. 2012. Measurement of mRNA abundance using RNA-seq data: RPKM measure is inconsistent among samples. *Theory Biosci* **131**: 281-285.

Zhang J, Rosenberg HF, Nei M. 1998. Positive Darwinian selection after gene duplication in primate ribonuclease genes. *Proc Natl Acad Sci USA* **95**: 3708-3713.